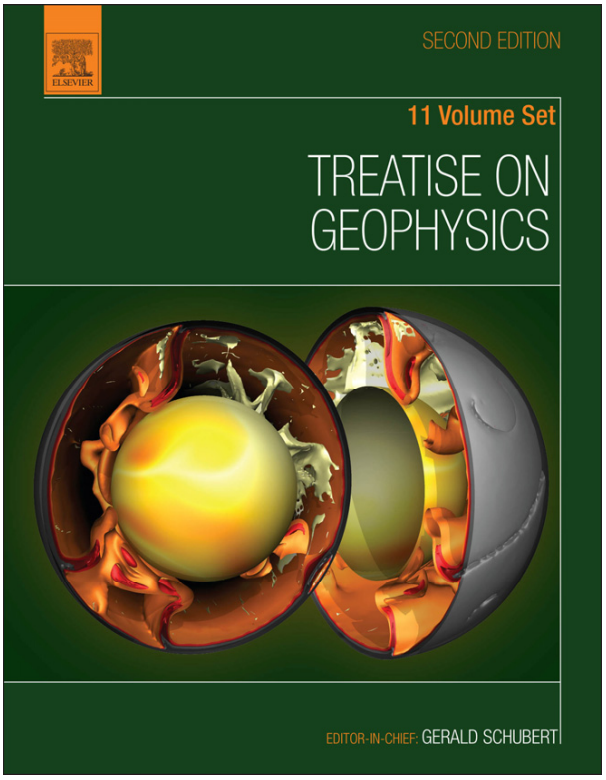

Jekeli C Potential Theory and the Static Gravity Field of the Earth. In: Gerald Schubert (editor-in-chief) Treatise on Geophysics, 2nd edition, Vol 3. Oxford: Elsevier; 2015. p. 9-35.

3.02 Potential Theory and the Static Gravity Field of the Earth

C Jekeli, The Ohio State University, Columbus, OH, USA

3.02.1 Introduction

Classical gravitational potential theory has its roots in the late renaissance period when the position of the Earth in the cosmos was established on modern scientific, observation-based grounds. A study of Earth's gravitational field is a study of Earth's mass including its transport in time and its influence on near objects; and, fundamentally, it is a geodetic study of Earth's shape, which is described largely (70%) by the surface of the oceans. This initial section provides a historical backdrop to Newtonian potential theory and introduces some concepts in physical geodesy that set the stage for later formulations.

3.02.1.1 Historical Notes

Gravitation is a physical phenomenon so pervasive and incidental that humankind generally has taken it for granted with scarcely a second thought. The Greek philosopher Aristotle (384–322 BC) allowed no more than to assert that gravitation is a natural property of material things that causes them to fall (or rise, in the case of some gases) and the more material, the greater the tendency to do so. It was enough of a self-evident explanation that it was not yet to receive the scrutiny of the scientific method, the beginnings of which, ironically, are credited to Aristotle. Almost two thousand years later, Galileo Galilei (1564–1642) finally took up the challenge to understand gravitation through observation and scientific investigation. His experimentally derived law of falling bodies corrected the Aristotelian view and divorced the effect of gravitation from the mass of the falling object – all bodies fall with the same acceleration. This truly monumental contribution to physics was, however, only a local explanation of how bodies behaved under gravitational influence. Johannes Kepler's (1571–1630) observations of planetary orbits pointed to other types of laws, principally an inverse-square law according to which bodies are attracted by forces that vary with the inverse square of distance. The genius of Isaac Newton (1642–1727) brought it all together in his *Philosophiæ Naturalis Principia Mathematica* of 1687 with a single and simple all-embracing law that in one bold stroke explained the dynamics of the entire universe (today, there is more to understanding the dynamics of the cosmos, but Newton's law remarkably holds its own). The mass of a body was again an essential aspect, not as a self-attribute as Aristotle had implied, but as the source of attraction for other bodies: each material body attracts every other material body according to a very specific rule (Newton's law of gravitation; see **Section 3.02.2**). Newton regretted that he could not explain exactly why mass has this property (as one still yearns to know today within the standard models of particle and quantum theories). Even Albert Einstein (1879–1955) in developing his general theory of relativity (i.e., the theory of gravitation) could only improve on Newton's theory by incorporating and explaining action at a distance (gravitational force acts with the speed of light as a fundamental tenet of the theory). Of course, Einstein did much more by reinterpreting gravitational attraction as a warping of space and time, which then allows consideration of gravitation effects at high velocity and due to great quantities of mass (e.g., black holes). However,

*Treatise on Geophysics, 2nd edition, (*2015), vol. 3, pp. 9-35

what actually mediates the gravitational effect still intensely occupies modern physicists and cosmologists.

Gravitation since its early scientific formulation initially belonged to the domain of astronomers, at least as far as the observable universe was concerned. Theory successfully predicted the observed perturbations of planetary orbits and even the location of previously unknown new planets (Neptune's discovery in 1846 based on calculations motivated by observed perturbations in Uranus' orbit was a major triumph for Newton's law). However, it was also ascertained by measurement that gravitational acceleration varies on Earth's surface, with respect to both altitude and latitude. Newton's law of gravitation again provided the backdrop for the variations observed with pendulums. An early achievement for his theory came when he successfully predicted the polar flattening in Earth's shape on the basis of hydrostatic equilibrium, which was confirmed finally (after some controversy) with geodetic measurements of long triangulated arcs in 1736–37 by Pierre-Louis Moreau de Maupertuis and Alexis-Claude Clairaut and independently by Pierre Bouguer, Louis Godin, and Charles Marie de La Condamine in 1739–1740. Gravitation thus already played an early role in geodesy, the science of determining the size and shape of the Earth, and came to dominate it through promulgation in large part by the father of modern geodesy, Friedrich R. Helmert (1843–1917).

Terrestrial gravitation through the twentieth century was considered a geodetic area of research, although, of course, its geophysical exploits should not be overlooked. But the advancement in modeling accuracy and global application was promoted mainly by geodesists who needed a well-defined reference for heights (a level surface) and whose astronomic observations of latitude and longitude needed to be corrected for the irregular direction of gravitation. Today, the modern view of a height reference for ordinary positioning is changing to that of a geometric, mathematical surface (an ellipsoid), and three-dimensional coordinates (latitude, longitude, and height) of points on the Earth's surface are readily obtained geometrically by ranging to the satellites of the Global Positioning System (GPS) or other Global Navigation System of Satellites (GNSSs).

The requirements of gravitation for GPS (GNSS) orbit determination within an Earth-centered coordinate system are now largely met with existing models. Improvements in gravitational models are motivated in geodesy primarily for rapid determination of traditional heights with respect to a level surface (the geoid). These heights, for example, the orthometric heights, in this sense then become derived attributes of points, rather than their cardinal components. They are essential for any hydrologic applications since they determine the flow of water. The relatively expensive and time-consuming traditional determination of heights by spirit leveling would be replaced by the combination of GPS (GNSS) heights above the ellipsoid and a model of the geoid (see also **Section 3.02.7**). Indeed, both Canada in 2013 and the United States (within a decade) plan to replace their vertical height data with a geoid determined strictly from a geopotential model (Huang and Véronneau, 2013; NGS, 2012).

Navigation and guidance exemplify a further specific niche where gravitation continues to find important relevance. While GPS dominates also this field, those vehicles requiring completely autonomous, self-contained systems must rely on inertial instruments (accelerometers and gyroscopes). These do not sense gravitation (see **Section 3.02.6.1**), yet gravitation contributes to the total definition of the vehicle trajectory, and thus, the output of inertial navigation systems must be compensated for the effect of gravitation. By far, the greatest emphasis in gravitation, however, has shifted to the Earth sciences, where detailed knowledge of the configuration of masses (the solid, liquid, and atmospheric components) and their transport and motion leads to improved understanding of the Earth systems (climate, hydrologic cycle, and tectonics) and their interactions with life. Oceanography, in particular, also requires a detailed knowledge of a level surface, the geoid, to model surface currents using satellite altimetry. Clearly, there is an essential temporal component in these studies, and, indeed, the temporal gravitational field holds center stage in many new investigations. Moreover, Earth's dynamic behavior influences point coordinates and Earth-fixed coordinate frames (Plag and Pearlman, 2009), and we come back to fundamental geodetic concerns in which the gravitational field plays an essential role!

This chapter deals with the static gravitational field. The theory of the potential from the classical Newtonian standpoint provides the foundation for modeling the field and thus deserves the focus of the exposition. The temporal part is a natural extension that is readily achieved with the addition of the time variable (no new laws are needed, if we neglect general relativistic effects) and will not be expounded here. We are primarily concerned with gravitation on and external to the solid and liquid Earth since this is the domain of most applications. The internal field can also be modeled for specialized purposes (such as submarine navigation), but internal geophysical modeling, for example, is done usually in terms of the sources (mass density distribution), rather than the resulting field.

3.02.1.2 Coordinate Systems

Modeling the Earth's gravitational field depends on the choice of a coordinate system. Customarily, owing to the Earth's general shape, a spherical polar coordinate system serves for most applications, and virtually all global models use these coordinates. However, the Earth is slightly flattened at the poles, and a spheroidal coordinate system has also been advocated for some near Earth applications. We note that the geodetic coordinates associated with a geodetic datum (based on an ellipsoid) are never used in a foundational sense to model the gravitational field since they do not admit to a separation-of-variables solution of Laplace's differential equation (**Section 3.02.4.1**).

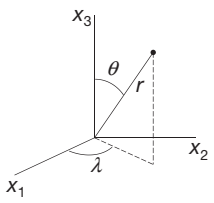

Figure 1 Spherical polar coordinates.

Spherical polar coordinates, described with the aid of Figure 1, comprise the spherical colatitude, θ; the longitude, λ; and the radial distance, r. Their relation to Cartesian coordinates is

$$\begin{aligned} x_1 &= r\sin\theta\cos\lambda \\ x_2 &= r\sin\theta\sin\lambda \\ x_3 &= r\cos\theta \end{aligned} \quad [1]$$

Considering Earth's polar flattening, a better approximation than a sphere of its mostly oceanic surface is an ellipsoid of revolution or spheroid (the term 'ellipsoid' is used here as conventionally used in physical geodesy). Such a surface is generated by rotating an ellipse about its minor axis, which is also the polar axis. The two focal points of the best-fitting, Earth-centered ellipsoid are located in the equator about $E = 522$ km from the center of the Earth. A given linear eccentricity, E, defines the corresponding set of coordinates, as described in Figure 2. The longitude is the same as in the spherical case. The colatitude, δ, is the complement of the so-called reduced latitude; and the distance coordinate, u, is the semiminor axis of the confocal ellipsoid through the point in question. We call (δ,λ,u) *spheroidal* coordinates; they are also known as Jacobi ellipsoidal coordinates, or sometimes simply ellipsoidal coordinates. Their relation to Cartesian coordinates is given by

$$\begin{aligned} x_1 &= \sqrt{u^2+E^2}\sin\delta\cos\lambda \\ x_2 &= \sqrt{u^2+E^2}\sin\delta\sin\lambda \\ x_3 &= u\cos\delta \end{aligned} \quad [2]$$

Points on Earth's best-fitting ellipsoid all have $u = b$; and all surfaces, $u =$ constant, are confocal ellipsoids (the analogy to the spherical case, when $E = 0$, should be evident). We note that these coordinates are not the same as Lamé's ellipsoidal coordinates for triaxial ellipsoids (Hobson, 1965).

3.02.1.3 Preliminary Definitions and Concepts

The gravitational potential, V, of the Earth is generated by its total mass density distribution. For applications on the Earth's surface, it is useful to include a potential-analogous function, ϕ, associated with the centrifugal acceleration due to Earth's rotation. The sum, $W = V + \phi$, is then known, in geodetic terminology, as the gravity potential, distinct from gravitational potential. The centrifugal potential, however, is not a Newtonian potential and is introduced for convenience only. It is further advantageous to define a relatively simple reference potential, or normal potential, that accounts for the bulk of the gravity potential (Section 3.02.5.2). The normal gravity potential, U, is defined as a gravity potential associated with a best-fitting ellipsoid, the normal ellipsoid, which rotates with the Earth and is also a surface of constant potential in this field. The difference between the actual and the normal gravity potentials is known as the disturbing potential: $T = W - U$; it thus excludes the centrifugal potential. The normal gravity potential accounts for approximately 99.9995% of the total potential.

The gradient of the potential is an acceleration, gravity, or gravitational acceleration, depending on whether or not it includes the centrifugal acceleration. Normal gravity, γ, comprises generally about 99.995% of the total gravity, g, although the difference in magnitudes, the gravity disturbance, δg, can be as large as several parts in 10^4. A special kind of difference, called the gravity anomaly, Δg, is defined as the difference between gravity at a point, P, and normal gravity at a corresponding point, Q, where $W_P = U_Q$ and P and Q are on the same perpendicular to the normal ellipsoid.

The surface of constant gravity potential, W_0, that closely approximates mean sea level is known as the geoid. If the constant normal gravity potential, U_0, on the normal ellipsoid is equal to the constant gravity potential of the geoid, then the gravity anomaly on the geoid is the difference between gravity on the geoid and normal gravity on the ellipsoid at respective points, P_0 and Q_0, sharing the same perpendicular to the ellipsoid. The separation between the geoid and the ellipsoid is known as the geoid undulation, N, or also the geoid height (Figure 3). A simple Taylor expansion of the normal gravity potential along the ellipsoid perpendicular yields the following important formula:

$$N = \frac{T}{\gamma} \quad [3]$$

This is Bruns' equation (Hofmann-Wellenhof and Moritz, 2005), which is accurate to a few millimeters in N and which can be extended to $N = T/\gamma - (W_0 - U_0)/\gamma$ for the general case, $W_0 \neq U_0$. The gravity anomaly (on the geoid) is the gravity disturbance corrected for the evaluation of normal gravity on the ellipsoid instead of the geoid. This correction is $N\partial\gamma/\partial h = (\partial\gamma/\partial h)(T/\gamma)$, where h is height along the ellipsoid perpendicular. We have approximately $\delta g = -\partial T/\partial h$ and hence

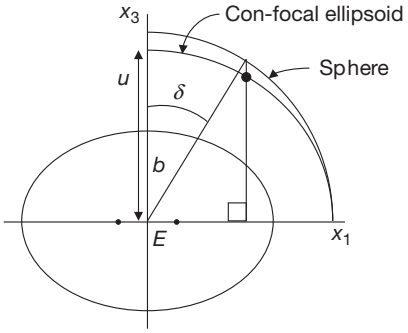

Figure 2 Ellipsoidal coordinates.

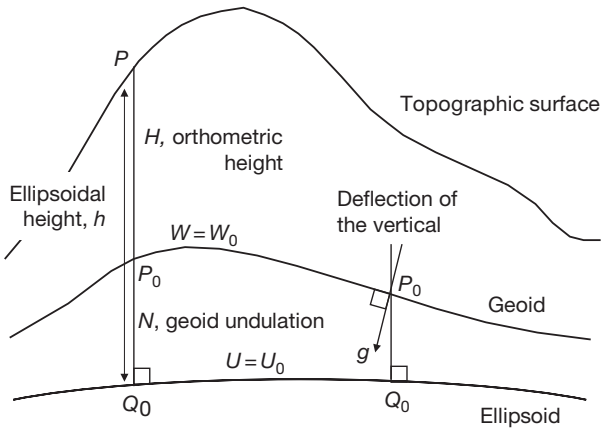

Figure 3 Relative geometry of geoid and ellipsoid.

$$\Delta g = -\frac{\partial T}{\partial h} + \frac{1}{\gamma}\frac{\partial \gamma}{\partial h}T \qquad [4]$$

which is known as the fundamental equation of physical geodesy (Hofmann-Wellenhof and Moritz, 2005).

The slope of the geoid with respect to the ellipsoid is also the angle between the corresponding perpendiculars to these surfaces. This angle is known as the deflection of the vertical, that is, the deflection of the plumb line (perpendicular to the geoid) relative to the perpendicular to the normal ellipsoid. The deflection angle has components, ξ and η, respectively, in the north and east directions. The spherical approximations to the gravity disturbance, the gravity anomaly, and the deflection of the vertical are given by (Hofmann-Wellenhof and Moritz, 2005)

$$\delta g = -\frac{\partial T}{\partial r}, \quad \Delta g = -\frac{\partial T}{\partial r} - \frac{2}{r}T,$$

$$\xi = \frac{1}{\gamma}\frac{\partial T}{r\partial \theta}, \quad \eta = -\frac{1}{\gamma}\frac{\partial T}{r\sin\theta\ \partial \lambda}, \qquad [5]$$

where the signs on the derivatives are a matter of convention.

3.02.2 Newton's Law of Gravitation

In its original form, Newton's law of gravitation applies only to idealized point masses. It describes the force of attraction, $\boldsymbol{F}$, experienced by two such solitary masses as being proportional to the product of the masses, m_1 and m_2; inversely proportional to the squared distance, ℓ^2, between them; and directed along the line joining them:

$$\boldsymbol{F} = G\frac{m_1 m_2}{\ell^2}\boldsymbol{n} \qquad [6]$$

where G is a constant, known as Newton's gravitational constant, that takes care of the units between the left- and right-hand sides of the equation; it can be determined by experiment, and the current internationally (2010 CODATA) accepted value is (Mohr et al., 2012)

$$G = (6.67384 \pm 0.00012) \times 10^{-11}\,\mathrm{m^3\,kg^{-1}\,s^{-2}} \qquad [7]$$

The unit vector $\boldsymbol{n}$ in eqn [6] is directed from either point mass to the other, and thus, the gravitational force is attractive and applies equally to one mass as the other. Newton's law of gravitation is universal as far as we know, breaking down when action at a distance cannot be assumed instantaneous and when very large velocities and masses are involved. Those cases must rely on Einstein's more comprehensive theory of general relativity, which describes gravitation as a characteristic curvature of the space–time continuum. In most geophysical and geodetic applications, the Newtonian theory is entirely adequate and it is the basis of the present exposition.

We can ascribe a gravitational acceleration to the gravitational force, which represents the acceleration that one mass undergoes due to the gravitational attraction of the other. Specifically, from the law of gravitation, we have (for point masses) the gravitational acceleration of m_1 due to the gravitational attraction of m_2:

$$\boldsymbol{g} = G\frac{m_2}{\ell^2}\boldsymbol{n} \qquad [8]$$

where the vector $\boldsymbol{g}$ is independent of the mass, m_1, of the body being accelerated (which Galileo found by experiment).

By the law of superposition, the gravitational force, or the gravitational acceleration, due to many point masses is the vector sum of the forces or accelerations generated by the individual point masses. Manipulating vectors in this way are certainly feasible, but fortunately, a more appropriate concept of gravitation as a scalar field simplifies the treatment of arbitrary mass distributions.

This more modern view of gravitation (already adopted by Gauss (1777–1855) and Green (1793–1841)) holds that it is a field having a gravitational potential. The concept of the gravitational field was fully developed by Lagrange (1736–1813) and Laplace (1749–1827), among others (Kellogg, 1953); and the potential, V, of the gravitational field is defined in terms of the gravitational acceleration, $\boldsymbol{g}$, that a test particle would undergo in the field according to the equation

$$\nabla V = \boldsymbol{g} \qquad [9]$$

where ∇ is the gradient operator (a vector of operators). Further elucidation of gravitation as a field grew from Einstein's attempt to incorporate gravitation into his special theory of relativity where no reference frame has special significance above all others. It was necessary to consider that gravitational force is not a real force (i.e., it is not an applied force, like friction or propulsion) – rather, it is known as a kinematic force, that is, one whose action is proportional to the mass on which it acts (like the centrifugal force) (Martin, 1988).

Though continuing with the classical Newtonian potential, we specifically interpret gravitation as an acceleration different from the acceleration induced by real, applied forces. This becomes especially important when considering the measurement of gravitation (**Section 3.02.6.1**). The gravitational potential, V, is a *scalar* function, and as defined here, V is derived directly on the basis of Newton's law of gravitation. To make it completely consistent with this law and thus declare it a Newtonian potential, we must impose the following conditions:

$$\lim_{\ell\to\infty} \ell V = Gm \quad \text{and} \quad \lim_{\ell\to\infty} V = 0 \qquad [10]$$

where m is the attracting mass and we say that the potential is regular at infinity. It is easy to show that the gravitational potential at any point in space due to a point mass, in order to satisfy eqns [8]–[10], must be

$$V = \frac{Gm}{\ell} \qquad [11]$$

where, again, ℓ is the distance between the mass and the point where the potential is expressed. Note that V for $\ell = 0$ does not exist in this case; that is, the field of a point mass has a singularity. We use here the convention that the potential is always positive (in contrast to physics, where it is usually defined to be negative, conceptually closer to potential energy).

Applying the law of superposition, the gravitational potential of many point masses is the sum of the potentials of the individual points (see **Figure 4**):

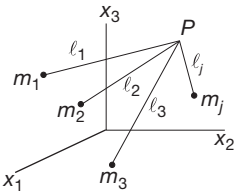

Figure 4 Discrete set of mass points (superposition principle).

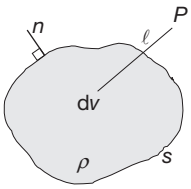

Figure 5 Continuous density distribution.

$$V_P = G\sum_j \frac{m_j}{\ell_j} \qquad [12]$$

For infinitely many points in a closed bounded region with infinitesimally small masses, dm, the summation in eqn [12] changes to an integration

$$V_P = G\int_{\text{mass}} \frac{dm}{\ell} \qquad [13]$$

or changing variables (i.e., units), $dm = \rho dv$, where ρ represents density (mass per volume) and dv is a volume element, we have (Figure 5)

$$V_P = G\iiint_{\text{volume}} \frac{\rho}{\ell} dv \qquad [14]$$

In eqn [14], ℓ is the distance between the evaluation point, P, and the point of integration. In spherical polar coordinates (Section 3.02.1.2), these points are (θ,λ,r) and (θ',λ',r'), respectively. The volume element in this case is given by $dv = r'^2 \sin\theta' \, d\lambda' \, d\theta' \, dr'$. V and its first derivatives are continuous everywhere – even in the case that P is on the bounding surface or inside the mass distribution, where there is the apparent singularity at $\ell = 0$. In this case, by changing to a coordinate system whose origin is at P, the volume element becomes $dv = \ell^2 \sin\psi \, d\alpha \, d\psi \, d\ell$ (for some different colatitude and longitude ψ and α); and, clearly, the singularity disappears – the integral is said to be weakly singular.

Suppose that the density distribution over the volume depends only on radial distance (from the center of mass): $\rho = \rho(r')$, and that P is an exterior evaluation point. The surface bounding the masses necessarily is a sphere (say, of radius, R), and because of the spherically symmetrical density, we may choose the integration coordinate system so that the polar axis passes through P. Then,

$$\ell = \sqrt{r'^2 + r^2 - 2r'r\cos\theta'}, \quad d\ell = \frac{1}{\ell} r' r \sin\theta' \, d\theta' \qquad [15]$$

It is easy to show that with this change of variables (from θ to ℓ), the integral [14] becomes simply

$$V(\theta,\lambda,r) = \frac{GM}{r}, \quad r \geq R \qquad [16]$$

where M is the total mass bounded by the sphere. This shows that to a very good approximation, the external gravitational potential of a planet such as the Earth (with concentrically layered density) is the same as that of a point mass.

The gravitational potential that is generated by other homogeneous bodies has been formulated in various ways, usually in terms of first and second spatial derivatives, conforming to gravitational measurements (Section 3.02.6), and in Cartesian coordinates. For example, Hofmann-Wellenhof and Moritz (2005) derived the expressions for the potential and its vertical derivative due to a cylinder along its axis. The following are expressions for the first and second derivatives of the potential due to a right rectangular prism with sides, $a_1 \leq x_1' \leq a_2$, $b_1 \leq x_2' \leq b_2$, and $c_1 \leq x_3' \leq c_2$, and valid in the exterior space. For $g_j = \partial V/\partial x_j$,

$$g_j = -G\rho\left(\left(x_k - x_k'\right)\ln\left(x_\ell - x_\ell' + r\right) + \left(x_\ell - x_\ell'\right)\ln\left(x_k - x_k' + r\right) - \left(x_j - x_j'\right)\tan^{-1}\frac{\left(x_k - x_k'\right)\left(x_\ell - x_\ell'\right)}{\left(x_j - x_j'\right)r}\right)\Bigg|_{x_1'=a_1}^{a_2}\Bigg|_{x_2'=b_1}^{b_2}\Bigg|_{x_3'=c_1}^{c_2} \qquad [17]$$

and for $\Gamma_{jk} = \partial^2 V/(\partial x_j \partial x_k)$,

$$\Gamma_{jj} = G\rho\tan^{-1}\frac{\left(x_k - x_k'\right)\left(x_\ell - x_\ell'\right)}{\left(x_j - x_j'\right)r}\Bigg|_{x_1'=a_1}^{a_2}\Bigg|_{x_2'=b_1}^{b_2}\Bigg|_{x_3'=c_1}^{c_2} \qquad [18]$$

$$\Gamma_{jk} = -G\rho\ln\left(x_\ell - x_\ell' + r\right)\Bigg|_{x_1'=a_1}^{a_2}\Bigg|_{x_2'=b_1}^{b_2}\Bigg|_{x_3'=c_1}^{c_2} \qquad [19]$$

where (x_1,x_2,x_3) is the point of computation and (j,k,ℓ) is a cyclic permutation of $(1,2,3)$. Formulas for general polyhedra may be found, for example, in Petrovic (1996) and Tsoulis and Petrovic (2001).

Besides volumetric mass (density) distributions, it is of interest to consider surface distributions. Imagine an infinitesimally thin layer of mass on a surface, s, where the units of density in this case are those of mass per area. Then, analogous to eqn [14], the potential is

$$V_P = G\iint_s \frac{\rho}{\ell} ds \qquad [20]$$

In this case, V is a continuous function everywhere, but its first derivatives are discontinuous at the surface. Or, one can imagine two infinitesimally close density layers (double layer or layer of mass dipoles), where the units of density are now those of mass per area times length. It turns out that the potential in this case is given by (see Heiskanen and Moritz, 1967)

$$V_P = G\iint_s \rho\frac{\partial}{\partial n}\left(\frac{1}{\ell}\right) ds \qquad [21]$$

where $\partial/\partial n$ is the directional derivative along the perpendicular to the surface (Figure 5). Now, V itself is discontinuous at the surface, as are all its derivatives. In all cases, V is a Newtonian potential, being derived from the basic formula [11] for a point mass that follows from Newton's law of gravitation (eqn [6]).

The following properties of the gravitational potential are useful for subsequent expositions. First, consider Stokes' theorem, for a vector function, f, defined on a surface, s:

$$\iint_s (\nabla \times f)\cdot \boldsymbol{n}\,\mathrm{d}s = \oint_p f\cdot \mathrm{d}\boldsymbol{r} \qquad [22]$$

where p is any closed path in the surface, $\boldsymbol{n}$ is the unit vector perpendicular to the surface, and $\mathrm{d}\boldsymbol{r}$ is a differential displacement along the path. From eqn [9], we find

$$\nabla \times \boldsymbol{g} = 0 \qquad [23]$$

since $\boldsymbol{\nabla} \times \boldsymbol{\nabla} = \mathbf{0}$; and hence, applying Stokes' theorem, we find that with $\boldsymbol{F} = m\boldsymbol{g}$,

$$w = \oint F\cdot \mathrm{d}\boldsymbol{s} = 0 \qquad [24]$$

That is, the gravitational field is conservative: the work, w, expended in moving a mass around a closed path in this field vanishes. In contrast, dissipating forces (real forces!), like friction, expend work or energy, which shows again the special nature of the gravitational force.

It can be shown (Kellogg, 1953, p. 156) that the second partial derivatives of a Newtonian potential, V, satisfy the following differential equation, known as Poisson's equation:

$$\nabla^2 V = -4\pi G\rho \qquad [25]$$

where $\nabla^2 = \boldsymbol{\nabla}\cdot\boldsymbol{\nabla}$ formally is the scalar product of two gradient operators and is called the Laplacian operator. In Cartesian coordinates, it is given by

$$\nabla^2 = \frac{\partial^2}{\partial x_1^2} + \frac{\partial^2}{\partial x_2^2} + \frac{\partial^2}{\partial x_3^2} \qquad [26]$$

Note that the Laplacian is a scalar operator. Equation [25] is a local characterization of the potential field, as opposed to the global characterization given by eqn [14]. Poisson's equation holds wherever the mass density, ρ, satisfies certain conditions similar to continuity (Hölder conditions, see Kellogg, 1953, pp. 152–153). A special case of eqn [25] applies for those points where the density vanishes (i.e., in free space); then, Poisson's equation turns into Laplace's equation:

$$\nabla^2 V = 0 \qquad [27]$$

It is easily verified that the point mass potential satisfies eqn [27]; that is,

$$\nabla^2\left(\frac{1}{\ell}\right) = 0 \qquad [28]$$

where $\ell = \sqrt{(x_1 - x_1')^2 + (x_2 - x_2')^2 + (x_3 - x_3')^2}$ and the mass point is at (x_1', x_2', x_3').

The solutions to Laplace's eqn [27] are known as harmonic functions; here, we also impose the conditions [10] on the solution, if it is a Newtonian potential and if the mass-free region includes infinity. Hence, every Newtonian potential is a harmonic function in free space. The converse is also true: every harmonic function can be represented as a Newtonian potential of a mass distribution (**Section 3.02.3.1**).

Whether as a volume or a layer density distribution, the corresponding potential is the sum or integral of the source value multiplied by the inverse distance function (or its normal derivative for the dipole layer). This function depends on both the source points and the computation point and is known as a Green's function. It is also known as the 'kernel' function of the integral representation of the potential. Functions of this type also play a dominant role in representing the potential as solutions to boundary-value problems (BVPs), as shown in subsequent sections.

This section concludes with another type of potential that finds uses in two-dimensional modeling. Many local geophysical density contrasts are long in one horizontal direction, such as faults and dikes, and may be characterized sufficiently in two dimensions, that is, with a single horizontal coordinate and the vertical coordinate. We start with the potential for an infinitesimally thin rod of finite length, $2c$, and parallel to the x_2-axis, whose standard Newtonian potential is

$$V = G\mu \int_{-c}^{c} \frac{\mathrm{d}x_2'}{\sqrt{(x_1 - x_1')^2 + (x_2 - x_2')^2 + (x_3 - x_3')^2}} \qquad [29]$$

where (x_1', x_3') is its offset from the origin (**Figure 6**) and μ is its constant line density. Taking the limit, $c \to \infty$, it can be shown that (up to a constant) the potential becomes (Kellogg, 1953, p. 56)

$$V = 2G\mu \ln\frac{1}{r} \qquad [30]$$

where $r = \sqrt{(x_1 - x_1')^2 + (x_3 - x_3')^2}$ is the distance of the computation point from the rod. This is sometimes referred to as the logarithmic potential. It is not a Newtonian potential since it does not vanish when $r \to \infty$ (see eqn [10]). If a long two-dimensional structure has a certain cross-sectional *shape* in the (x_1', x_3') plane, then its potential may be approximated by

$$V = 2G \iint_{\text{shape}} \mu \ln\frac{1}{r}\,\mathrm{d}x_1'\,\mathrm{d}x_3' \qquad [31]$$

and the derivatives follow easily for simple structures (see, e.g., Telford et al., 1990).

3.02.3 Boundary-Value Problems

If the density distribution of the Earth's interior and the boundary of the volume were known, then the problem of determining the Earth's gravitational potential field is solved by the volume integral of eqn [14]. In reality, of course, we do not have access to this information, at least not the density, with sufficient detail. The Preliminary Reference Earth Model, of Dziewonsky and Anderson (1981), still in use today by geophysicists, represents a good profile of Earth's radial density, but does not attempt to model in detail the lateral density heterogeneities. On the other hand, efforts to model the crust, especially at active tectonic plate margins where their dynamics is associated with earthquakes and mountain formation, often

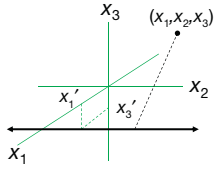

Figure 6 Geometry for the potential of a long rod.

rely (in addition to seismological data) on gravity data that are inverted to constrain the density distribution. Thus, gravity models, in principle, are developed not from three-dimensional density integrals, but from measurements on or above the Earth's surface. In this section, we see how the problem of determining the exterior gravitational potential can be reconstructed in terms of surface integrals, thus depending exclusively (at least in theory) on these measurements.

3.02.3.1 Green's Identities

Formally, eqn [27] represents a partial differential equation for V. Solving this equation is the essence of the determination of the Earth's external gravitational potential through potential theory. Like any differential equation, a complete solution is obtained only with the application of boundary conditions, that is, imposing values on the solution that it must assume at a boundary of the region in which it is valid. In our case, the boundary is the Earth's surface and the exterior space is where eqn [27] holds (the atmosphere and other celestial bodies are neglected or mathematically removed from the problem using corrections to the boundary values). In order to study the solutions to these BVPs, that is, to show that solutions exist and are unique, we take advantage of some very important theorems and identities. It is noted that only a rather elementary introduction to BVPs is offered here with no attempt to address the much larger field of solutions to partial differential equations.

The first, seminal result is Gauss' divergence theorem (analogous to Stokes' theorem, eqn [22]):

$$\iiint_v \nabla\cdot f \,\mathrm{d}v = \iint_s f_n \,\mathrm{d}s \qquad [32]$$

where f is an arbitrary (differentiable) vector function and $f_n = \boldsymbol{n}\cdot f$ is the component of f along the outward unit normal vector, $\boldsymbol{n}$ (see Figure 5). The surface, s, encloses the volume, v. Equation [32] says that the sum of how much f changes throughout the volume, that is, the net effect, ultimately, is equivalent to the sum of its values projected orthogonally with respect to the surface. Conceptually, a volume integral thus can be replaced by a surface integral, which is important since the gravitational potential is due to a volume density distribution that we do not know, but we do have access to gravitational quantities on a surface by way of measurements.

Equation [32] applies to general vector functions that have continuous first derivatives. In particular, let U and V be two scalar functions having continuous second derivatives; and consider the vector function $f = U\boldsymbol{\nabla}V$. Then, since $\boldsymbol{n}\cdot\boldsymbol{\nabla} = \partial/\partial n$, and

$$\boldsymbol{\nabla}\cdot(U\boldsymbol{\nabla}V) = \boldsymbol{\nabla}U\cdot\boldsymbol{\nabla}V + U\nabla^2 V \qquad [33]$$

we can apply Gauss' divergence theorem to get Green's first identity:

$$\iiint_v (\boldsymbol{\nabla}U\cdot\boldsymbol{\nabla}V + U\nabla^2 V)\,\mathrm{d}v = \iint_s U\frac{\partial V}{\partial n}\,\mathrm{d}s \qquad [34]$$

Interchanging the roles of U and V in eqn [34], one obtains a similar formula, which when subtracted from eqn [34] yields Green's second identity:

$$\iiint_v (U\nabla^2 V - V\nabla^2 U)\,\mathrm{d}v = \iint_s \left(U\frac{\partial V}{\partial n} - V\frac{\partial U}{\partial n}\right)\mathrm{d}s \qquad [35]$$

and which is valid for any U and V with continuous derivatives up to second order.

Now, let $U = 1/\ell$, where ℓ is the usual distance between an integration point and an evaluation point. And, suppose that the volume, v, is the space exterior to the Earth (i.e., Gauss' divergence theorem applies to any volume, not just volumes containing a mass distribution). With reference to Figure 7, consider the evaluation point, P, to be inside the volume (free space) that is bounded by the surface, s; P is thus outside the Earth's surface. Let V be a solution to eqn [27], that is, it is the gravitational potential of the Earth. From the volume, v, exclude the volume bounded by a small sphere, σ, centered at P. This sphere becomes part of the surface that bounds the volume, v. Then, since U, by our definition, is a point mass potential, $\nabla^2 U = 0$ everywhere in v (which excludes the interior of the small sphere around P); and the second identity [35] gives

$$\iint_s \left(\frac{1}{\ell}\frac{\partial V}{\partial n} - V\frac{\partial}{\partial n}\left(\frac{1}{\ell}\right)\right)\mathrm{d}s + \iint_\sigma \left(\frac{1}{\ell}\frac{\partial V}{\partial n} - V\frac{\partial}{\partial n}\left(\frac{1}{\ell}\right)\right)\mathrm{d}\sigma = 0 \qquad [36]$$

The unit vector, $\boldsymbol{n}$, represents the perpendicular pointing away from v. On the small sphere, $\boldsymbol{n}$ is opposite in direction to $\ell = r$, and the second integral becomes

$$\begin{aligned}\iint_\sigma \left(-\frac{1}{r}\frac{\partial V}{\partial r} + V\frac{\partial}{\partial r}\left(\frac{1}{r}\right)\right)\mathrm{d}\sigma &= -\iint_\Omega \frac{1}{r}\frac{\partial V}{\partial r}r^2\,\mathrm{d}\Omega - \iint_\Omega V\,\mathrm{d}\Omega \\ &= -\iint_\Omega \frac{\partial V}{\partial r}r\,\mathrm{d}\Omega - 4\pi\overline{V}\end{aligned} \qquad [37]$$

where $\mathrm{d}\sigma = r^2\mathrm{d}\Omega$; Ω is the solid angle, 4π; and $\overline{V}$ is an average value of V on σ. Now, in the limit as the radius of the small sphere shrinks to zero, the right-hand side of eqn [37] approaches $0 - 4\pi V_P$. Hence, eqn [36] becomes (Kellogg, 1953, p. 219)

$$V_P = \frac{1}{4\pi}\iint_s \left(\frac{1}{\ell}\frac{\partial V}{\partial n} - V\frac{\partial}{\partial n}\left(\frac{1}{\ell}\right)\right)\mathrm{d}s \qquad [38]$$

with $\boldsymbol{n}$ pointing down (away from the space outside the Earth). This is a special case of Green's third identity. A change in sign of the right-side transforms $\boldsymbol{n}$ to a normal unit vector pointing into v, away from the masses, which conforms more to an Earth-centered coordinate system.

The right side of eqn [38] is the sum of single- and double-layer potentials and thus shows that every harmonic

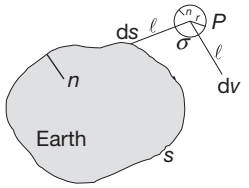

Figure 7 Geometry for special case of Green's third identity.

function (i.e., a function that satisfies Laplace's equation) can be written as a Newtonian potential. Equation [38] is also a solution to a BVP; in this case, the boundary values are independent values of V and of its normal derivative, both on s (Cauchy problem). In the succeeding text and in Section 3.02.4.1, we encounter another BVP (Robin problem) in which the potential and its normal derivative are given in a specified linear combination on s. Using a similar procedure and with some extra care, it can be shown (see also Courant and Hilbert, 1962, vol. 2, p. 256 (footnote)) that if P is on the surface, then

$$V_P = \frac{1}{2\pi}\iint_s \left(\frac{1}{\ell}\frac{\partial V}{\partial n} - V\frac{\partial}{\partial n}\left(\frac{1}{\ell}\right)\right) ds \qquad [39]$$

where $\boldsymbol{n}$ points into the masses. Comparing this to eqn [38], we see that V is discontinuous as one approaches the surface; this is due to the double-layer part (see eqn [21]).

Equation [38] demonstrates that a solution to a particular BVP exists. Specifically, we are able to measure the potential (up to a constant) and its derivatives (the gravitational acceleration) on the surface and thus have a formula to compute the potential anywhere in exterior space, provided that we also know the surface, s. Other BVPs also have solutions under appropriate conditions; a discussion of existence theorems is beyond the present scope and may be found in Kellogg (1953, Chapter 1.13). Equation [39] has deep geodetic significance. One objective of geodesy is to determine the shape of the Earth's surface. If we have measurements of gravitational quantities on the Earth's surface, then conceptually we are able to determine its shape from eqn [39], where it would be the only unknown quantity. This is the basis behind the work of Molodensky et al. (1962) to which we return briefly at the end of this section.

3.02.3.2 Uniqueness Theorems

Often the existence of a solution is proved simply by finding one (as illustrated earlier). Whether such as solution is the only one depends on a corresponding uniqueness theorem. That is, we wish to know if a certain set of boundary values will yield just one potential in space. Before considering such theorems, we classify the BVPs that are typically encountered when determining the exterior potential from measurements on a boundary. In all cases, it is an exterior BVP; that is, the gravitational potential, V, is harmonic ($\nabla^2 V = 0$) in the space exterior to a closed surface that contains all the masses. The exterior space thus contains infinity. Interior BVPs can be constructed, as well, but are not applicable to our objectives:

- Dirichlet problem (or BVP of the first kind): solve for V in the exterior space, given its values everywhere on the boundary.
- Neumann problem (or BVP of the second kind): solve for V in the exterior space, given values of its normal derivative everywhere on the boundary.
- Robin problem (mixed BVP or BVP of the third kind): solve for V in the exterior space, given a linear combination of it and its normal derivative on the boundary.

Using Green's identities, we prove the following theorems for these exterior problems; similar results hold for the interior problems.

Theorem 1 *If V is harmonic (hence continuously differentiable) in a closed region, v, and if V vanishes everywhere on the boundary, s, then V also vanishes everywhere in the region, v.*

Proof: Since $V = 0$ on s, Green's first identity (eqn [34]) with $U = V$ gives

$$\iiint_v (\boldsymbol{\nabla} V)^2 dv = \iint_s V\frac{\partial V}{\partial n} ds = 0 \qquad [40]$$

where the integral on the left side is, therefore, always zero; and the integrand is always nonnegative. Hence, it must vanish, $\nabla V = 0$, everywhere in v, which implies that $V =$ constant in v. Since V is continuous in v and $V = 0$ on s, that constant must be zero; and so, $V = 0$ in v.

This theorem solves the Dirichlet problem for the trivial case of zero boundary values, and it enables the following uniqueness theorem for the general Dirichlet problem.

Theorem 2 (Stokes' theorem) *If V is harmonic (hence continuously differentiable) in a closed region, v, then V is uniquely determined in v by its values on the boundary, s.*

Proof: Suppose the determination is not unique: that is, suppose there are V_1 and V_2 both harmonic in v and both having the same boundary values on s. Then, the function $V = V_2 - V_1$ is harmonic in v with all boundary values equal to zero. Hence, by Theorem 1, $V_2 - V_1 = 0$ identically in v, or $V_2 = V_1$ everywhere, which implies that any determination is unique based on the boundary values.

Theorem 3 *If V is harmonic (hence continuously differentiable) in the exterior region, v, with closed boundary, s, then V is uniquely determined by the values of its normal derivative on s.*

Proof: We begin with Green's first identity (eqn [34]) as in the proof of Theorem 1 to show that if the normal derivative vanishes everywhere on s, then V is a constant in v. Now, suppose there are two harmonic functions in v, V_1 and V_2, with the same normal derivative values on s. Then, the normal derivative values of their difference are zero; and by the aforementioned demonstration, $V = V_2 - V_1 =$ constant in v. Since V is a Newtonian potential in the exterior space, that constant is zero, since by eqn [10], $\lim_{\ell\to\infty} V = 0$. Thus, $V_2 = V_1$, and the boundary values determine the potential uniquely.

This is a uniqueness theorem for the exterior Neumann BVP. Solutions to the interior problem are unique only up to an arbitrary constant.

Theorem 4 *Suppose V is harmonic (hence continuously differentiable) in the closed region, v, with boundary, s; and suppose the boundary values are given by*

$$g = \alpha V|_s + \beta\left.\frac{\partial V}{\partial n}\right|_s \qquad [41]$$

then, V is uniquely determined by these values if $\alpha/\beta > 0$.

Proof: Suppose there are two harmonic functions, V_1 and V_2, with the same boundary values, g, on s. Then, $V = V_2 - V_1$ is harmonic with boundary values

$$\alpha(V_2 - V_1)|_s + \beta\left(\frac{\partial V_2}{\partial n} - \frac{\partial V_1}{\partial n}\right)\Big|_s = 0 \qquad [42]$$

where, with $U = V = V_2 - V_1$, Green's first identity (eqn [34]) gives

$$\iiint_v (\nabla(V_2 - V_1))^2 \mathrm{d}v = \iint_s (V_2 - V_1)\frac{-\alpha}{\beta}(V_2 - V_1)\mathrm{d}s \qquad [43]$$

Then,

$$\iiint_v (\nabla(V_2 - V_1))^2 \mathrm{d}v + \frac{\alpha}{\beta}\iint_S (V_2 - V_1)^2 \mathrm{d}S = 0 \qquad [44]$$

and since $\alpha/\beta > 0$, eqn [44] implies that $\nabla(V_2 - V_1) = 0$ in v; and $V_2 - V_1 = 0$ on s. Hence, $V_2 - V_1 =$ constant in v; and $V_2 = V_1$ on s. By the continuity of V_1 and V_2, the constant must be zero; and the uniqueness is proved.

The solution to the Robin problem is thus unique only in certain cases. The most famous problem in physical geodesy is the determination of the disturbing potential, T, from gravity anomalies, Δg, on the geoid (**Section 3.02.1.3**). Suppose T is harmonic outside the geoid; the second of eqn [5] provides an approximate form of boundary condition, showing that this is a type of Robin problem. We find that $\alpha = -2/r$; and recalling that when v is the exterior space, the unit vector $\boldsymbol{n}$ points inward toward the masses, that is, $\partial/\partial n = -\partial/\partial r$, we get $\beta = 1$. Thus, the condition in Theorem 4 on α/β is not fulfilled and the uniqueness is not guaranteed. In fact, we will see that the solution obtained for the spherical boundary is arbitrary with respect to the coordinate origin (**Section 3.02.4.1**).

3.02.3.3 Solutions by Integral Equation

Green's identities show how a solution to Laplace's equation can be transformed from a volume integral, that is, an integral of source points, to a surface integral of boundary-value points, as demonstrated by eqn [38]. The uniqueness theorems for the BVPs suggest that the potential due to a volume density distribution can also be represented as due to a generalized density layer on the bounding surface, as long as the result is harmonic in exterior space, satisfies the boundary conditions, and is regular at infinity like a Newtonian potential. Molodensky et al. (1962) supposed that the disturbing potential is expressible as

$$T = \iint_s \frac{\mu}{\ell}\mathrm{d}s \qquad [45]$$

where μ is a surface density to be solved using the boundary condition. With the spherical approximation for the gravity anomaly (eqn [5]), one arrives at the following integral equation:

$$2\pi\mu\cos\zeta - \iint_s \left(\frac{\partial}{\partial r}\left(\frac{1}{\ell}\right) + \frac{2}{r\ell}\right)\mu\,\mathrm{d}s = \Delta g \qquad [46]$$

The first term accounts for the discontinuity at the surface of the derivative of the potential of a density layer, where ζ is the deflection angle between the normal to the surface and the direction of the (radial) derivative (Günter, 1967, p. 69; Heiskanen and Moritz, 1967, p. 6). This Fredholm integral equation of the second kind can be simplified with further approximations; and a solution for the density, μ, ultimately leads to the solution for the disturbing potential (Moritz, 1980).

Other forms of representing the potential have also been investigated, where Green's functions other than $1/\ell$ lead to simplifications of the integral equation (e.g., Petrovskaya, 1979). Nevertheless, most practical solutions rely on approximations, such as the spherical approximation for the boundary condition, and even the formulated solutions are not strictly guaranteed to converge to the true solutions (Moritz, 1980). Further treatments of the BVP in a geodetic/mathematical setting may be found in the volume edited by Sansò and Rummel (1997).

In the next section, we consider solutions for T as surface integrals of boundary values with appropriate Green's functions and spherical boundaries. In other words, the boundary values (whether of the first, second, or third kind) may be thought of as sources and the consequent potential is again the sum (integral) of the product of a boundary value and an appropriate Green's function (i.e., a function that depends on both the source point and the computation point in some form of inverse distance in accordance with Newtonian potential theory). Solutions are readily obtained because the boundary is a sphere.

3.02.4 Solutions to the Spherical BVP

This section develops two types of solutions to standard BVPs when the boundary is a sphere: the spherical harmonic series and an integral with a Green's function. All three types of problems are solved, but emphasis is put on the third BVP since gravity anomalies are the most prevalent boundary values (on land, at least). In addition, it is shown how Green's function integrals can be inverted to obtain, for example, gravity anomalies from values of the potential, now considered as boundary values. Not all possible inverse relationships are given, but it should be clear at the end that, in principle, virtually any gravitational quantity can be obtained in space from any other quantity on the spherical boundary.

3.02.4.1 Spherical Harmonics and Green's Functions

For simple boundaries, Laplace's equation [27] is relatively easy to solve provided that there is an appropriate coordinate system. For the Earth, the solutions commonly rely on approximating the boundary by a sphere. This case is described in detail and a more accurate approximation based on an ellipsoid of revolution is briefly examined in **Section 3.02.5.2** for the normal potential. In spherical polar coordinates, (θ,λ,r), the Laplacian operator is given by (Hobson, 1965, p. 9)

$$\nabla^2 = \frac{1}{r^2}\frac{\partial}{\partial r}\left(r^2\frac{\partial}{\partial r}\right) + \frac{1}{r^2}\frac{1}{\sin\theta}\frac{\partial}{\partial\theta}\left(\sin\theta\frac{\partial}{\partial\theta}\right) + \frac{1}{r^2\sin^2\theta}\frac{\partial^2}{\partial\lambda^2} \qquad [47]$$

A solution to $\nabla^2 V = 0$ in the space outside a sphere of radius, R, with center at the coordinate origin can be found by the method of separation of variables, whereby one postulates the form of the solution, V, as

$$V(\theta,\lambda,r) = f(\theta)g(\lambda)h(r) \qquad [48]$$

Substituting this and the Laplacian, eqn [47], into eqn [27], the multivariate partial differential equation separates into three univariate ordinary differential equations (Hobson, 1965, p. 9; Morse and Feshbach, 1953, p. 1264). Their solutions are well-known functions, for example,

$$V(\theta,\lambda,r) = P_{nm}(\cos\theta)\sin m\lambda\frac{1}{r^{n+1}} \quad \text{or}$$
$$V(\theta,\lambda,r) = P_{nm}(\cos\theta)\cos m\lambda\frac{1}{r^{n+1}} \qquad [49]$$

where $P_{nm}(t)$ is the associated Legendre function of the first kind and n and m are integers such that $0 \le m \le n$ and $n \ge 0$. Other solutions are also possible (e.g., $g(\lambda) = e^{a\lambda}$ $(a \varepsilon \mathbb{R})$ and $h(r) = r^n$), but only eqn [49] is consistent with the problem at hand: to find a real-valued Newtonian potential for the exterior space of the Earth (regular at infinity and 2π-periodic in longitude). The general solution is a linear combination of solutions of the forms given by eqn [49] for all possible integers, n and m, and can be written compactly as

$$V(\theta,\lambda,r) = \sum_{n=0}^{\infty}\sum_{m=-n}^{n}\left(\frac{R}{r}\right)^{n+1} v_{nm}\overline{Y}_{nm}(\theta,\lambda) \qquad [50]$$

where the $\overline{Y}_{nm}$ are surface spherical harmonic functions defined as

$$\overline{Y}_{nm}(\theta,\lambda) = \overline{P}_{n|m|}(\cos\theta)\begin{cases}\cos m\lambda, & m \ge 0\\ \sin|m|\lambda, & m < 0\end{cases} \qquad [51]$$

and $\overline{P}_{nm}$ is a normalization of P_{nm} so that the orthogonality of the spherical harmonics is simply

$$\frac{1}{4\pi}\iint_{\sigma}\overline{Y}_{nm}(\theta,\lambda)\overline{Y}_{n'm'}(\theta,\lambda)\mathrm{d}\sigma = \begin{cases}1, & n = n' \text{ and } m = m'\\ 0, & n \ne n' \text{ or } m \ne m'\end{cases} \qquad [52]$$

and where $\sigma = \{(\theta,\lambda)|0 \le \theta \le \pi,\ 0 \le \lambda \le 2\pi\}$ represents the unit sphere, with $\mathrm{d}\sigma = \sin\theta\,\mathrm{d}\theta\,\mathrm{d}\lambda$. For a complete mathematical treatment of spherical harmonics, one may refer to Müller (1966). The bounding spherical radius, R, is introduced so that all the constant coefficients, v_{nm}, sometimes known as Stokes' constants (Section 3.02.5.1), have identical units of measure. Applying the orthogonality to the general solution [50], these coefficients can be determined if the function, V, is known on the bounding sphere (boundary condition):

$$v_{nm} = \frac{1}{4\pi}\iint_{\sigma}V(\theta,\lambda,R)\overline{Y}_{nm}(\theta,\lambda)\mathrm{d}\sigma \qquad [53]$$

Equation [50] is known as a spherical harmonic expansion of V, and with eqn [53], it represents a solution to the Dirichlet BVP if the boundary is a sphere. The solution thus exists and is unique in the sense that these boundary values generate no other potential. We will, however, find another equivalent form of the solution.

In a more formal mathematical setting, the solution [52] is an infinite linear combination of orthogonal basis functions (eigenfunctions), and the coefficients, v_{nm}, are the corresponding eigenvalues. One may also interpret the set of coefficients as the spectrum (Legendre spectrum) of the potential on the sphere of radius, R (analogous to the Fourier spectrum of a function on the plane or line). The integers, n and m, correspond to wave numbers and are called degree (n) and order (m), respectively. The spherical harmonics are further classified as zonal ($m = 0$), meaning that the zeros of $\overline{Y}_{n0}$ divide the sphere into latitudinal zones; sectorial ($m = n$), where the zeros of $\overline{Y}_{nn}$ divide the sphere into longitudinal sectors; and tesseral (the zeros of $\overline{Y}_{nm}$ tessellate the sphere) (Figure 8).

While the spherical harmonic series has its advantages in global representations and spectral interpretations of the field, a Green's function representation provides a more local characterization of the field. That is, changing a boundary value anywhere on the globe changes all coefficients, v_{nm}, according to eqn [53], which poses a numerical challenge both in applications and in keeping a standard model up-to-date. However, since Green's function essentially depends on the inverse distance (or higher powers thereof), a remote change in boundary value generally does not appreciably affect the local determination of the field.

When the boundary is a sphere, the solutions to the BVPs using a Green's function are easily derived from the spherical harmonic series representation. Moreover, it is possible to derive additional integral relationships (with appropriate Green's functions) among all the derivatives of the potential. To formalize and simultaneously simplify these derivations, consider harmonic functions, f and h, where h depends only

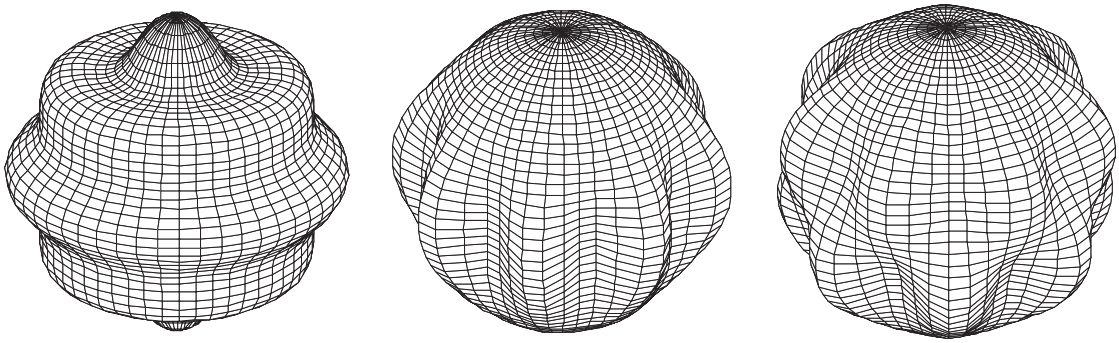

Figure 8 Examples of zonal, sectorial, and tesseral harmonics on the sphere.

on θ and r, and the function g, defined on the sphere of radius, R. Thus, let

$$f(\theta,\lambda,r)=\sum_{n=0}^{\infty}\sum_{m=-n}^{n}\left(\frac{R}{r}\right)^{n+1}f_{nm}\overline{Y}_{nm}(\theta,\lambda),\quad r\geq R \qquad [54]$$

$$h(\theta,r)=\sum_{n=0}^{\infty}(2n+1)\left(\frac{R}{r}\right)^{n+1}h_nP_n(\cos\theta),\quad r\geq R \qquad [55]$$

$$g(\theta,\lambda,R)=\sum_{n=0}^{\infty}\sum_{m=-n}^{n}g_{nm}\overline{Y}_{nm}(\theta,\lambda) \qquad [56]$$

where $P_n(\cos\theta)=\overline{P}_{n0}(\cos\theta)/\sqrt{2n+1}$ is the nth-degree Legendre polynomial. Constants f_{nm} and g_{nm} are the respective harmonic coefficients of f and g when these functions are restricted to the sphere of radius, R. Then, using the decomposition formula for Legendre polynomials,

$$P_n(\cos\psi)=\frac{1}{2n+1}\sum_{m=-n}^{n}\overline{Y}_{nm}(\theta,\lambda)\overline{Y}_{nm}\left(\theta',\lambda'\right) \qquad [57]$$

where

$$\cos\psi=\cos\theta\cos\theta'+\sin\theta\sin\theta'\cos\left(\lambda-\lambda'\right) \qquad [58]$$

it is easy to prove the following theorem.

Theorem 5 (convolution theorem in spectral analysis on the sphere)

$$f(\theta,\lambda,r)=\frac{1}{4\pi}\iint_{\sigma}g\left(\theta',\lambda',R\right)h(\psi,r)\mathrm{d}\sigma \quad \text{if and only if}$$

$$f_{nm}=g_{nm}h_n \qquad [59]$$

where here and in the following, $\mathrm{d}\sigma=\sin\theta'\,\mathrm{d}\theta'\,\mathrm{d}\lambda'$. The angle, ψ, is the distance on the unit sphere between points (θ,λ) and (θ',λ').

Proof: The forward statement [59] follows directly by substituting eqns [55] and [57] into the first eqn [59], together with the spherical harmonic expansion [56] for g. A comparison with the spherical harmonic expansion for f yields the result. All steps in this proof are reversible, and so, the reverse statement also holds.

Consider now f to be the potential, V, on and outside the sphere of radius, R, and its restriction to the sphere to be the function, $g(\theta,\lambda)=V(\theta,\lambda,R)$. Then, since $g_{nm}=f_{nm}$, we have $h_n=1$, for all n; and by Theorem 5

$$V(\theta,\lambda,r)=\frac{1}{4\pi}\iint_{\sigma}V\left(\theta',\lambda',R\right)U(\psi,r)\mathrm{d}\sigma \qquad [60]$$

where

$$U(\psi,r)=\sum_{n=0}^{\infty}(2n+1)\left(\frac{R}{r}\right)^{n+1}P_n(\cos\psi) \qquad [61]$$

For the distance,

$$\ell=\sqrt{r^2+R^2-2rR\cos\psi} \qquad [62]$$

between points (θ,λ,r) and (θ',λ',R), with $r\geq R$, the identity (the *Coulomb expansion*; Cushing, 1975, p. 155)

$$\frac{1}{\ell}=\frac{1}{R}\sum_{n=0}^{\infty}\left(\frac{R}{r}\right)^{n+1}P_n(\cos\psi) \qquad [63]$$

yields after some arithmetic (based on taking the derivative on both sides with respect to r)

$$U(\psi,r)=\frac{R(r^2-R^2)}{\ell^3} \qquad [64]$$

Solutions [50] and [60] to the Dirichlet BVP for a spherical boundary are identical in view of the convolution theorem [59]. The integral in [60] is known as *Poisson's integral*, and the function U is the corresponding Green's function, also known as Poisson's kernel.

For convenience, one separates Earth's gravitational potential into a reference potential (**Section 3.02.1.3**) and the disturbing potential, T. The disturbing potential is harmonic in free space and satisfies Poisson's integral if the boundary is a sphere. In deference to physical geodesy where relationships between the disturbing potential and its derivatives are routinely applied, the following derivations are developed in terms of T but hold equally for any exterior Newtonian potential. Let

$$T(\theta,\lambda,r)=\frac{GM}{R}\sum_{n=0}^{\infty}\sum_{m=-n}^{n}\left(\frac{R}{r}\right)^{n+1}\delta C_{nm}\overline{Y}_{nm}(\theta,\lambda) \qquad [65]$$

where M is the total mass (including the atmosphere) of the Earth and the δC_{nm} are unit-less harmonic coefficients, being also the differences between coefficients for the total and reference gravitational potentials (**Section 3.02.5.2**). The coefficient, δC_{00}, is zero under the assumption that the reference field accounts completely for the central part of the total field. Note also that these coefficients specifically refer to the sphere of radius, R, that is, they constitute the (normalized) spectrum of T on this sphere.

The gravity disturbance is defined in spherical approximation to be the negative radial derivative of T, the first of eqn [5]. From eqn [65], we have

$$\begin{aligned}\delta g(\theta,\lambda,r)&=-\frac{\partial}{\partial r}T(\theta,\lambda,r)\\&=\frac{GM}{R^2}\sum_{n=0}^{\infty}\sum_{m=-n}^{n}\left(\frac{R}{r}\right)^{n+2}(n+1)\delta C_{nm}\overline{Y}_{nm}(\theta,\lambda)\end{aligned} \qquad [66]$$

and applying the convolution theorem [59] to $f(\theta,\lambda,r)=T(\theta,\lambda,r)$ and $g(\theta,\lambda,R)=R\delta g(\theta,\lambda,R)$, we obtain

$$T(\theta,\lambda,r)=\frac{R}{4\pi}\iint_{\sigma}\delta g\left(\theta',\lambda',R\right)H(\psi,r)\mathrm{d}\sigma \qquad [67]$$

where with $g_{nm}=GM(n+1)\delta C_{nm}/R$ and $f_{nm}=GM\delta C_{nm}$, we have $h_n=f_{nm}/g_{nm}=R/(n+1)$ and hence

$$H(\psi,r)=\sum_{n=0}^{\infty}\frac{2n+1}{n+1}\left(\frac{R}{r}\right)^{n+1}P_n(\cos\psi) \qquad [68]$$

The integral in [67] is known as the *Hotine integral*, Green's function, H, is called the Hotine kernel, and with a derivation based on eqn [63], it is given by (Hotine, 1969, p. 311)

$$H(\psi,r)=\frac{2R}{\ell}-\ln\left(\frac{R+\ell-r\cos\psi}{r(1-\cos\psi)}\right) \qquad [69]$$

Equation [67] solves the Neumann BVP when the boundary is a sphere.

The gravity anomaly, again, in spherical approximation is defined by (eqn [5])

$$\Delta g(\theta,\lambda,r) = \left(-\frac{\partial}{\partial r} - \frac{2}{r}\right) T(\theta,\lambda,r) \qquad [70]$$

or also

$$\Delta g(\theta,\lambda,r) = \frac{GM}{R^2}\sum_{n=0}^{\infty}\sum_{m=-n}^{n}\left(\frac{R}{r}\right)^{n+2}(n-1)\delta C_{nm}\overline{Y}_{nm}(\theta,\lambda) \qquad [71]$$

where in this case, we have $g_{nm} = GM(n-1)\delta C_{nm}/R$ and $h_n = R/(n-1)$. The convolution theorem then leads to the geodetically famous *Stokes' integral*:

$$T(\theta,\lambda,r) = \frac{R}{4\pi}\iint_{\sigma}\Delta g\left(\theta',\lambda',R\right)S(\psi,r)\mathrm{d}\sigma \qquad [72]$$

where we *define* the corresponding Green's function

$$S(\psi,r) = \sum_{n=2}^{\infty}\frac{2n+1}{n-1}\left(\frac{R}{r}\right)^{n+1}P_n(\cos\psi) = 2\frac{R}{\ell} + \frac{R}{r} - 3\frac{R\ell}{r^2} - 5\frac{R^2}{r^2}\cos\psi - 3\frac{R^2}{r^2}\cos\psi\ln\frac{\ell + r - R\cos\psi}{2r} \qquad [73]$$

more commonly called Stokes' kernel. Equation [72] solves the Robin BVP if the boundary is a sphere, but it includes specific constraints that ensure the solution's uniqueness – the solution by itself is not unique, in this case, as proved in Section 3.02.3.2. Indeed, eqn [71] shows that the gravity anomaly has no first-degree harmonics that for the disturbing potential, therefore, cannot be determined from the boundary values. Conventionally, Stokes' kernel also excludes the zero-degree harmonic, and thus, the complete solution for the disturbing potential is given by

$$T(\theta,\lambda,r) = \frac{GM}{r}\delta C_{00} + \frac{GM}{R}\sum_{m=-1}^{1}\left(\frac{R}{r}\right)^{2}\delta C_{1m}\overline{Y}_{1m}(\theta,\lambda) + \frac{R}{4\pi}\iint_{\sigma}\Delta g\left(\theta',\lambda',R\right)S(\psi,r)\mathrm{d}\sigma \qquad [74]$$

The central term, δC_{00}, is proportional to the difference in GM of the Earth and of the reference ellipsoid and is zero to high accuracy. The first-degree harmonic coefficients, δC_{1m}, are proportional to the center of mass coordinates and can also be set to zero with appropriate definition of the coordinate system (see Section 3.02.5.1). Thus, Stokes' integral [72] is the more common expression for the disturbing potential, but it embodies hidden constraints.

We note that gravity anomalies can also serve as boundary values in the harmonic series form of the solution for the disturbing potential. Applying the orthogonality of the spherical harmonics to eqn [71] yields immediately

$$\delta C_{nm} = \frac{R^2}{4\pi(n-1)GM}\iint_{\sigma}\Delta g\left(\theta',\lambda',R\right)\overline{Y}_{nm}\left(\theta',\lambda'\right)\mathrm{d}\sigma, \quad n \geq 2 \qquad [75]$$

A similar formula holds when gravity disturbances are the boundary values ($n-1$ in the denominator changes to $n+1$). In either case, the boundary values formally are assumed to reside on a sphere of radius, R. An approximation results if they are given on the geoid, as is usually the case.

The two solutions to the Robin BVP (Section 3.02.3.2) with boundary values defined by eqn [70], one given by eqn [72] and the other by eqns [65] and [75], are equivalent. Similar to Poisson's integral, eqn [72] may be viewed more as a local representation since Stokes' function, $S(\psi,r)$, attenuates significantly with distance from the computation point. Equation [65], on the other hand, is a global representation, where the harmonic coefficients, δC_{nm}, may also be determined from other boundary values, for example, *in situ* satellite measurements or from satellite tracking data (Section 3.02.6.1). In practice, the two solutions are combined in order to reduce the error when necessarily limiting the integral of the latter to a local neighborhood. One removes a global model (finite series) from the gravity anomalies and subsequently restores the model to the disturbing potential. This remove–restore technique is discussed in Section 3.02.6.2.

3.02.4.2 Inverse Stokes' and Hotine Integrals

The convolution integrals in the previous section can easily be inverted by considering again the spectral relationships. For the gravity anomaly in space, we note that $f = r\Delta g$ is harmonic with coefficients, $f_{nm} = GM(n-1)\delta C_{nm}/R$. Letting $g = T|_{r=R}$ with $g_{nm} = GM\delta C_{nm}/R$, we find that $h_n = n-1$; and by the convolution theorem, we can write

$$\Delta g(\theta,\lambda,r) = \frac{1}{4\pi R}\iint_{\sigma}T\left(\theta',\lambda',R\right)\hat{Z}(\psi,r)\mathrm{d}\sigma \qquad [76]$$

where

$$\hat{Z}(\psi,r) = \sum_{n=0}^{\infty}(2n+1)(n-1)\left(\frac{R}{r}\right)^{n+2}P_n(\cos\psi) \qquad [77]$$

The zero- and first-degree terms are included provisionally. Note that

$$\hat{Z}(\psi,r) = -R\left(\frac{\partial}{\partial r} + \frac{2}{r}\right)U(\psi,r) \qquad [78]$$

That is, we could have simply used the Dirichlet solution [60] to obtain the gravity anomaly, as given by [76], from the disturbing potential. It is convenient to separate the kernel function as follows:

$$\hat{Z}(\psi,r) = Z(\psi,r) - \sum_{n=0}^{\infty}(2n+1)\left(\frac{R}{r}\right)^{n+2}P_n(\cos\psi) \qquad [79]$$

where

$$Z(\psi,r) = \sum_{n=1}^{\infty}(2n+1)n\left(\frac{R}{r}\right)^{n+2}P_n(\cos\psi) \qquad [80]$$

and we find that with eqn [60] applied to T,

$$\Delta g(\theta,\lambda,r) = -\frac{1}{r}T(\theta,\lambda,r) + \frac{1}{4\pi R}\iint_{\sigma}T\left(\theta',\lambda',R\right)Z(\psi,r)\,\mathrm{d}\sigma \qquad [81]$$

Now, since Z has no zero-degree harmonics, its integral over the sphere vanishes, and one can write the numerically more convenient formula:

$$\Delta g(\theta,\lambda,r) = -\frac{1}{r}T(\theta,\lambda,r) + \frac{1}{4\pi R}\iint_{\sigma}\left(T\left(\theta',\lambda',R\right) - T(\theta,\lambda,R)\right)Z(\psi,r)\,\mathrm{d}\sigma \quad [82]$$

This is the inverse Stokes' formula. Given T on the sphere of radius R, for example, in the form of geoid undulations, $T=\gamma N$, this form is useful when the gravity anomaly is also desired on this sphere. It is one way to determine gravity anomalies on the ocean surface from satellite altimetry, which yields N directly, given the position of the satellite. Analogously, from eqns [66] and [70], it is readily seen that the inverse Hotine formula is given by

$$\delta g(\theta,\lambda,r) = \frac{1}{r}T(\theta,\lambda,r) + \frac{1}{4\pi R}\iint_{\sigma}\left(T\left(\theta',\lambda',R\right) - T(\theta,\lambda,R)\right)Z(\psi,r)\,\mathrm{d}\sigma \quad [83]$$

Note that the sum of eqns [82] and [83] yields the approximate relationship between the gravity disturbance and the gravity anomaly inferred from eqn [5]. A closed expression for Z may be obtained by writing $(2n+1)n=(n+1)(n+2)+n(n+1)-3(n+1)+1$ and combining appropriate derivatives of eqn [63]:

$$Z(\psi,r) = \frac{R^2}{\ell^5}\left(\frac{\ell^4}{r} + \ell^2(5R\cos\psi - r) - 6rR^2\sin^2\psi\right) \quad [84]$$

Finally, we realize that, for $r=R$, the series for $Z(\psi,R)$ is not uniformly convergent and special numerical procedures (that are outside the present scope) are required to approximate the corresponding integrals.

3.02.4.3 Vening-Meinesz Integral and Its Inverse

Other derivatives of the disturbing potential may also be determined from boundary values. We consider here only gravity anomalies, being the most prevalent data type on land areas. The solution is in the form of either a series – simply the derivative of the series [65] with coefficients given by eqn [75] – or an integral with appropriate derivative of Green's function. The horizontal derivatives of the disturbing potential may be interpreted as the deflections of the vertical to which they are proportional in spherical approximation (eqn [5]):

$$\begin{Bmatrix}\xi(\theta,\lambda,r)\\ \eta(\theta,\lambda,r)\end{Bmatrix} = \frac{1}{\gamma(\theta,r)}\begin{Bmatrix}\frac{1}{r}\frac{\partial}{\partial\theta}\\ -\frac{1}{r\sin\theta}\frac{\partial}{\partial\lambda}\end{Bmatrix}T(\theta,\lambda,r) \quad [85]$$

where ξ,η are the north and east deflection components, respectively, and γ is the normal gravity. Clearly, the derivatives can be taken directly inside Stokes' integral, and we find

$$\begin{Bmatrix}\xi(\theta,\lambda,r)\\ \eta(\theta,\lambda,r)\end{Bmatrix} = \frac{R}{4\pi r\gamma(\theta,r)}\iint_{\sigma}\Delta g\left(\theta',\lambda',R\right)\frac{\partial}{\partial\psi}S(\psi,r)\begin{Bmatrix}\cos\alpha\\ \sin\alpha\end{Bmatrix}\mathrm{d}\sigma \quad [86]$$

where

$$\begin{Bmatrix}\frac{1}{r}\frac{\partial}{\partial\theta}\\ -\frac{1}{r\sin\theta}\frac{\partial}{\partial\lambda}\end{Bmatrix} = \frac{1}{r}\begin{Bmatrix}\frac{\partial\psi}{\partial\theta}\\ -\frac{1}{\sin\theta}\frac{\partial\psi}{\partial\lambda}\end{Bmatrix}\frac{\partial}{\partial\psi} \quad [87]$$

and

$$\frac{\partial\psi}{\partial\theta} = \frac{1}{\sin\psi}\left(\sin\theta\cos\theta' - \cos\theta\sin\theta'\cos\left(\lambda-\lambda'\right)\right) = \cos\alpha$$
$$-\frac{1}{\sin\theta}\frac{\partial\psi}{\partial\lambda} = \frac{1}{\sin\psi}\sin\theta'\sin\left(\lambda'-\lambda\right) = \sin\alpha \quad [88]$$

where the angle, α, is the azimuth of (θ',λ') at (θ,λ) on the unit sphere. The integrals [86] are known as the *Vening-Meinesz integrals*. Analogous integrals for the deflections arise when the boundary values are the gravity disturbances (Green's functions are then derivatives of the Hotine kernel).

For the inverse Vening-Meinesz integrals, we need to make use of Green's first identity for surface functions, f and g:

$$\iint_{s} f\Delta^*(g)\,\mathrm{d}s + \iint_{s}\boldsymbol{\nabla}f\cdot\boldsymbol{\nabla}g\,\mathrm{d}s = \int_{b} f\boldsymbol{\nabla}g\cdot\boldsymbol{n}\,\mathrm{d}b \quad [89]$$

where b is the boundary (a line) of a surface, s; $\boldsymbol{\nabla}$ and Δ^* are the gradient and Laplace–Beltrami operators, which for the sphere are given by

$$\boldsymbol{\nabla} = \begin{pmatrix}\frac{\partial}{\partial\theta}\\ \frac{1}{\sin\theta}\frac{\partial}{\partial\lambda}\end{pmatrix}, \quad \Delta^* = \frac{\partial^2}{\partial\theta^2} + \cot\theta\frac{\partial}{\partial\theta} + \frac{1}{\sin^2\theta}\frac{\partial^2}{\partial\lambda^2} \quad [90]$$

and $\boldsymbol{n}$ is the unit vector normal to b. For a closed surface such as the sphere, the line integral vanishes, and we have

$$\iint_{\sigma} f\Delta^*(g)\mathrm{d}\sigma = -\iint_{\sigma}\boldsymbol{\nabla}f\cdot\boldsymbol{\nabla}g\;\mathrm{d}\sigma \quad [91]$$

The surface spherical harmonics, $\overline{Y}_{nm}(\theta,\lambda)$, satisfy the following differential equation:

$$\Delta^*\overline{Y}_{nm}(\theta,\lambda) + n(n+1)\overline{Y}_{nm}(\theta,\lambda) = 0 \quad [92]$$

and, therefore, the harmonic coefficients of $-\Delta^*T(\theta,\lambda,r)$ on the sphere of radius, R, are

$$g_{nm} \equiv \left[-\Delta^*T(\theta,\lambda,r)\right]_{nm} = n(n+1)\frac{GM}{R}\delta C_{nm} \quad [93]$$

Hence, by the convolution theorem (again, considering the harmonic function, $f=r\Delta g$),

$$\Delta g(\theta,\lambda,r) = -\frac{1}{4\pi R}\iint_{\sigma}\Delta^*T\left(\theta',\lambda',R\right)W(\psi,r)\mathrm{d}\sigma \quad [94]$$

where, since $f_{nm}=GM(n-1)\delta C_{nm}/R$,

$$W(\psi,r) = \sum_{n=2}^{\infty}\frac{(2n+1)(n-1)}{n(n+1)}\left(\frac{R}{r}\right)^{n+2}P_n(\cos\psi) \quad [95]$$

and where the zero-degree term of the gravity anomaly must be treated separately (e.g., it is set to zero in this case). Using Green's identity [91] and eqns [85], [87], and [88], we have

$$\Delta g(\theta,\lambda,r) = \frac{1}{4\pi R}\iint_{\sigma} \nabla T\left(\theta',\lambda',R\right)\cdot\nabla W(\psi,r)\mathrm{d}\sigma$$
$$= \frac{\gamma_0}{4\pi}\iint_{\sigma}\left(\xi\left(\theta',\lambda',R\right)\cos\alpha+\eta\left(\theta',\lambda',R\right)\sin\alpha\right)$$
$$\frac{\partial}{\partial\psi}W(\psi,r)\mathrm{d}\sigma \qquad [96]$$

where normal gravity on the sphere of radius, R, is approximated as a constant: $\gamma(\theta,R)\simeq\gamma_0$. Equation [96] represents a second way to compute gravity anomalies from satellite altimetry, where the along-track and cross-track altimetric differences are used to approximate the deflection components (with appropriate rotation to north and east components). Employing differences in altimetric measurements benefits the estimation since systematic errors, such as orbit error, cancel out. To speed up the computations, the problem is reformulated in the spectral domain; see, for example, Sandwell and Smith (1996).

Clearly, following the same procedure for $f=T$, we also have the following relationship:

$$T(\theta,\lambda,r) = \frac{R\gamma_0}{4\pi}\iint_{\sigma}\left(\xi\left(\theta',\lambda',R\right)\cos\alpha+\eta\left(\theta',\lambda',R\right)\sin\alpha\right)$$
$$\frac{\partial}{\partial\psi}B(\psi,r)\mathrm{d}\sigma \qquad [97]$$

where

$$B(\psi,r) = \sum_{n=2}^{\infty}\frac{(2n+1)}{n(n+1)}\left(\frac{R}{r}\right)^{n+1}P_n(\cos\psi) \qquad [98]$$

It is interesting to note that instead of an integral over the sphere, the inverse relationship between the disturbing potential on the sphere and the deflection of the vertical on the same sphere is also more straightforward in terms of a line integral:

$$T(\theta,\lambda,R) = T(\theta_0,\lambda_0,R) + \frac{\gamma_0}{4\pi}\int_{(\theta_0,\lambda_0)}^{(\theta,\lambda)}\left(\xi\left(\theta',\lambda',R\right)\mathrm{d}s_\theta-\eta\left(\theta',\lambda',R\right)\mathrm{d}s_\lambda\right) \qquad [99]$$

where

$$\mathrm{d}s_\theta = R\,\mathrm{d}\theta,\quad \mathrm{d}s_\lambda = R\sin\theta\ \mathrm{d}\lambda \qquad [100]$$

3.02.4.4 Concluding Remarks

The spherical harmonic series [65] represents the general solution to the exterior potential, regardless of the way the coefficients are determined. We know how to compute those coefficients exactly on the basis of a BVP, if the boundary is a sphere. More complicated boundaries would require corrections or, if these are omitted, would imply an approximation. If the coefficients are determined accurately (e.g., from satellite observations (**Section 3.02.6.1**), but not according to eqn [75]), then the spherical harmonic series model for the potential is not a spherical approximation. The spherical approximation enters when approximate relations such as eqn [5] are used and when the boundary is approximated as a sphere. However determined, the infinite series converges uniformly for all $r>R_c$, where R_c is the radius of the sphere that encloses all terrestrial masses (the *Brillouin sphere*). It may also converge in some sense below this sphere but would represent the true potential only in free space (above the Earth's surface, where Laplace's equation holds). In practice, though, convergence, per se, is not an issue since the series must be truncated at some finite degree. Any trend toward divergence is then part of the overall model error.

Model errors exist in all Green's function integrals as they depend on spherical approximations in the boundary condition. In addition, the surface of integration in these formulas is formally assumed to be the geoid (where normal derivatives of the potential coincide with gravity magnitude), but it is approximated as a sphere. The spherical approximation results, in the first place, from a neglect of the ellipsoid flattening, which is about 0.3% for the Earth. When working with the disturbing potential, this level of error was easily tolerated in the past (e.g., if the geoid undulation is 30 m, the spherical approximation accounts for about 10 cm error), but today, it requires attention as geoid undulation accuracy of 1 cm is pursued.

Green's functions all have singularities when the evaluation point is on the sphere of radius, R. For points above this sphere, it is easily verified that all the harmonic series for Green's functions converge uniformly, since $|P_n(\cos\psi)|\leq 1$. When $r=R$, the corresponding singularities of the integrals are either weak (Stokes' integral) or strong (e.g., Poisson's integral), requiring in the latter case special definition of the integral as a Cauchy principal value.

It is noted that the BVP solutions also require that no masses reside above the geoid (the boundary approximated as a sphere). To satisfy this condition, the topographic masses must be redistributed appropriately by mathematical reduction, and the gravity anomalies or disturbances measured on the Earth's surface must be reduced to the geoid. The mass redistribution must then be undone (mathematically), resulting in an indirect effect, in order to obtain the correct potential on or above the geoid. Details of these various procedures are found in Heiskanen and Moritz (1967, **Chapter 1.04**). The most common methodology today is the Helmert condensation method (Hofmann-Wellenhof and Moritz, 2005), whereby the topographic masses with assumed constant density are 'condensed' as a surface layer on the geoid, thus satisfying the conditions of the BVP. While this reduction has no particular geophysical interpretation, its indirect effect is generally smaller than for other reductions. The atmosphere, having significant mass, also affects gravity anomalies as a function of elevation. This effect may also be removed prior to using them as boundary values in the integral formulas (Moritz, 2000).

Finally, solutions to the BVP for the potential in *spheroidal* coordinates and ellipsoid boundary (see **Section 3.02.5.2**) replace the spherical approximation with a significantly improved ellipsoidal approximation, but there is no corresponding convolution theorem, as in eqn [59]. That is, integral solutions with analytic forms of a Green's function do not exist in this case because the inverse distance now depends on two surface coordinates. However, approximations have been formulated for all three types of BVP (see Yu et al., 2002 and references therein). In practice, solutions such as Stokes' integral (eqn [72]) still find general usage, especially if the

long-wavelength field is accommodated by a global model (remove–restore technique, Section 3.02.6.2) and where corrections are applied to reduce the spherical approximation error (e.g., Fei and Sideris, 2000).

3.02.5 Low-Degree Harmonics: Interpretation and Reference

The low-degree spherical harmonics of the Earth's gravitational potential lend themselves to interpretation with respect to the most elemental distribution of the Earth's density, which also leads to fundamental geometric characterizations, particularly for the second-degree harmonics. Let

$$C_{nm}^{(a)} = \frac{a}{GM}\left(\frac{R}{a}\right)^{n+1} v_{nm} \qquad [101]$$

be unit-less coefficients that refer to a sphere of radius, a. (Recall that coefficients, v_{nm} (eqn [50]), refer to a sphere of radius, R.) Relative to the central harmonic coefficient, $C_{00}^{(a)} = 1$, the next significant harmonic, $C_{20}^{(a)}$, for the Earth is more than three orders of magnitude smaller; and the remaining harmonic coefficients are at least two to three orders of magnitude smaller than that. The attenuation after degree two is much more gradual (Table 1), indicating that the bulk of the potential can be described by an ellipsoidal field. The normal gravitational field is such a field, but it also adheres to a geodetic definition that requires the underlying ellipsoid to be an equipotential surface in the corresponding normal gravity field. This section examines the low-degree harmonics from these two perspectives of interpretation and reference.

3.02.5.1 Low-Degree Harmonics as Density Moments

Returning to the general expression for the gravitational potential in terms of the Newtonian density integral (eqn [14]), and substituting the spherical harmonic series for the reciprocal distance (eqn [63] with [57]),

$$V(\theta,\lambda,r) = G\iiint_v \rho \frac{1}{r'}\sum_{n=0}^{\infty}\left(\frac{r'}{r}\right)^{n+1}\left(\frac{1}{2n+1}\sum_{m=-n}^{n}\overline{Y}_{nm}(\theta,\lambda)\overline{Y}_{nm}\left(\theta',\lambda'\right)\right)\mathrm{d}v$$
$$= \sum_{n=0}^{\infty}\sum_{m=-n}^{n}\left(\frac{R}{r}\right)^{n+1}\left(\frac{G}{R^{n+1}(2n+1)}\iiint_{\text{volume}}\rho\left(r'\right)^{n}\overline{Y}_{nm}\left(\theta',\lambda'\right)\mathrm{d}v\right)$$
$$\overline{Y}_{nm}(\theta,\lambda) \qquad [102]$$

yields a multipole expansion (so called from electrostatics) of the potential. The spherical harmonic coefficients, also commonly called Stokes' constants or coefficients in this case, are multipoles of the density distribution (cf., eqn [50]):

$$v_{nm} = \frac{G}{R^{n+1}(2n+1)}\iiint_v \rho\left(r'\right)^{n}\overline{Y}_{nm}\left(\theta',\lambda'\right)\mathrm{d}v \qquad [103]$$

One may also consider the nth-order moments of density (from the statistics of distributions) defined by

$$\mu_{\alpha\beta\gamma}^{(n)} = \iiint_v \left(x'\right)^{\alpha}\left(y'\right)^{\beta}\left(z'\right)^{\gamma}\rho\,\mathrm{d}v, \quad n = \alpha+\beta+\gamma \qquad [104]$$

(where, clearly risking confusion, we defer to the common nomenclature of order for the moments and degree for the spherical harmonics. Also for notational convenience, here, we use (x,y,z) for the Cartesian coordinates instead of (x_1, x_2, x_3) used in previous sections.) The multipoles of degree n and the moments of order n are related, although not all $(n+1)(n+2)/2$ moments of order n can be determined from the $2n+1$ multipoles of degree n, when $n \geq 2$. This indeterminacy is directly connected to the inability to determine the density distribution uniquely from external measurements of the potential (Chao, 2005), which is the classic geophysical inverse problem.

The zero-degree Stokes' coefficient is coordinate-invariant and is proportional to the total mass of the Earth:

$$v_{00} = \frac{G}{R}\iiint_v \rho\,\mathrm{d}v = \frac{GM}{R} \qquad [105]$$

and, it also represents a mass monopole, and it is proportional to the zeroth moment of the density, M.

The first-degree harmonic coefficients (representing dipoles) are proportional to the coordinates of the center of mass, (x_{cm},y_{cm},z_{cm}), which are proportional to the first-order moments of the density, as verified by recalling the definition of the first-degree spherical harmonics:

$$v_{1m} = \frac{G}{\sqrt{3}R^2}\iiint_v \rho\begin{Bmatrix} r'\sin\theta'\sin\lambda', & m=-1 \\ r'\cos\theta', & m=0 \\ r'\sin\theta'\cos\lambda', & m=1 \end{Bmatrix}\mathrm{d}v$$
$$= \frac{GM}{\sqrt{3}R^2}\begin{Bmatrix} y_{cm}, & m=-1 \\ z_{cm}, & m=0 \\ x_{cm}, & m=1 \end{Bmatrix} \qquad [106]$$

Nowadays, by tracking satellites, we have access to the center of mass of the Earth (including its atmosphere) since it defines the center of their orbits. Ignoring the small motion of the center of mass (annual amplitude of several millimeters) due to the temporal variations in the mass distribution, we may choose the coordinate origin for the geopotential model to coincide with the center of mass, thus annihilating the first-degree coefficients.

Table 1 Spherical harmonic coefficients of the total gravitational potential[a]

Degree, n	*Order*, m	$C_{nm}^{(a)}$	$C_{n,-m}^{(a)}$
2	0	−4.84170E−04	0.0
2	1	−2.39832E−10	1.42489E−09
2	2	2.43932E−06	−1.40028E−06
3	0	9.57189E−07	0.0
3	1	2.03048E−06	2.48172E−07
3	2	9.04802E−07	−6.19006E−07
3	3	7.21294E−07	1.41437E−06
4	0	5.39992E−07	0.0
4	1	−5.36167E−07	−4.73573E−07
4	2	3.50512E−07	6.62445E−07
4	3	9.90868E−07	−2.00976E−07
4	4	−1.88472E−07	3.08827E−07

[a]GRACE model GGM02S (Tapley et al., 2005).

The second-order density moments likewise are related to the second-degree harmonic coefficients (quadrupoles). They also define the inertia tensor of the body. The inertia tensor is the proportionality factor in the equation that relates the angular momentum vector, H, and the angular velocity, $\boldsymbol{\omega}$, of a body, like the Earth

$$\mathrm{H} = I\boldsymbol{\omega} \qquad [107]$$

and is denoted by

$$I = \begin{pmatrix} I_{xx} & I_{xy} & I_{xz} \\ I_{yx} & I_{yy} & I_{yz} \\ I_{zx} & I_{zy} & I_{zz} \end{pmatrix} \qquad [108]$$

It comprises the moments of inertia on the diagonal

$$\begin{aligned} I_{xx} &= \iiint_v \rho\left(y'^2 + z'^2\right) \mathrm{d}v, \quad I_{yy} \\ &= \iiint_v \rho\left(z'^2 + x'^2\right) \mathrm{d}v, \quad I_{zz} = \iiint_v \rho\left(x'^2 + y'^2\right) \mathrm{d}v \end{aligned} \qquad [109]$$

and the products of inertia off the diagonal

$$\begin{aligned} I_{xy} = I_{yx} &= -\iiint_v \rho\ x'y'\, \mathrm{d}v, \quad I_{xz} = I_{zx} \\ &= -\iiint_v \rho\ x'z'\, \mathrm{d}v, \quad I_{yz} = I_{zy} = -\iiint_v \rho\ y'z'\, \mathrm{d}v \end{aligned} \qquad [110]$$

Note that

$$I_{xx} = \mu^{(2)}_{020} + \mu^{(2)}_{002}, \quad I_{xy} = -\mu^{(2)}_{110} \text{ etc.}, \qquad [111]$$

and there are as many (six) independent tensor components as second-order density moments. Using the explicit expressions for the second-degree spherical harmonics, we have from eqn [103] with $n=2$

$$\begin{aligned} &v_{2,-2} = -\frac{\sqrt{15}\,G}{5R^3} I_{xy}, \quad v_{2,-1} = -\frac{\sqrt{15}\,G}{5R^3} I_{yz}, \quad v_{2,1} = -\frac{\sqrt{15}\,G}{5R^3} I_{xz} \\ &v_{2,0} = \frac{\sqrt{5}\,G}{10R^3}\left(I_{xx} + I_{yy} - 2I_{zz}\right), \quad v_{2,2} = \frac{\sqrt{15}\,G}{10R^3}\left(I_{yy} - I_{xx}\right) \end{aligned} \qquad [112]$$

which are also known as *MacCullagh's* formulas. Not all density moments (or moments of inertia) can be determined from these five Stokes' coefficients.

If the coordinate axes are chosen so as to diagonalize the inertia tensor (products of inertia are then equal to zero), then they are known as principal axes of inertia, or also 'figure' axes. For the Earth, the z-figure axis is very close to the spin axis (within several meters at the pole); both axes move with respect to each other and the Earth's surface (known as polar motion), with combinations of various periods (daily, monthly, annually, etc.) and secularly in a wandering fashion. Because of these motions, the figure axis is not useful as a coordinate axis that defines a frame fixed to the crust of the Earth. However, because of the proximity of the figure axis to the defined reference z-axis, the second-degree, first-order harmonic coefficients of the geopotential are relatively small (Table 1).

The arbitrary choice of the x-axis of our Earth-fixed reference coordinate system certainly did not attempt to eliminate the product of inertia, I_{xy} (the x-axis is defined by the intersection of the Greenwich meridian with the equator; and the y-axis completes a right-handed mutually orthogonal triad). However, it is possible to determine where the equatorial figure axis is located by combining values of the second-degree, second-order harmonic coefficients. Let u, v, and w be the axes that define a coordinate system in which the inertia tensor is diagonal; and assume that $I_{ww}=I_{zz}$. Let λ_0 be the longitude of the u-figure axis in our conventional (x,y,z) system. A rotation by the angle, $-\lambda_0$, about the w-(also z-)figure axis brings this ideal coordinate system back to the conventional one in which we calculate the harmonic coefficients. Tensors transform under rotation, defined by matrix, $\mathcal{R}$, according to

$$I_{xyz} = \mathcal{R}\, I_{uvw} \mathcal{R}^{\mathrm{T}} \qquad [113]$$

where the subscript on I denotes the coordinate system to which it refers. With the rotation about the w-axis given by the matrix

$$\mathcal{R} = \begin{pmatrix} \cos\lambda_0 & -\sin\lambda_0 & 0 \\ \sin\lambda_0 & \cos\lambda_0 & 0 \\ 0 & 0 & 1 \end{pmatrix} \qquad [114]$$

and with eqn [112], it is straightforward to show that

$$\begin{aligned} v_{2,-2} &= -\frac{\sqrt{15}\,G}{10R^3}\left(I_{uu} - I_{vv}\right) \sin 2\lambda_0 \\ v_{2,2} &= -\frac{\sqrt{15}\,G}{10R^3}\left(I_{uu} - I_{vv}\right) \cos 2\lambda_0 \end{aligned} \qquad [115]$$

Hence, we have

$$\lambda_0 = \frac{1}{2} \tan^{-1} \frac{v_{2,-2}}{v_{2,2}} \qquad [116]$$

where the quadrant is determined by the signs of the harmonic coefficients. From Table 1, we find that $\lambda_0 = -14.929°$; that is, the u-figure axis is in the mid-Atlantic between South America and Africa.

The second-degree, second-order harmonic coefficient, $v_{2,2}$, indicates the asymmetry of the Earth's mass distribution with respect to the equator. Since $v_{2,2}>0$ (for the Earth), eqn [115] shows that $I_{vv}>I_{uu}$ and thus the equator 'bulges' more in the direction of the u-figure axis; conversely, the equator is flattened in the direction of the v-figure axis. This flattening is relatively small: 1.1×10^{-5}.

Finally, consider the most important second-degree harmonic coefficient, the second zonal harmonic, $v_{2,0}$. Irrespective of the x-axis definition, it is proportional to the difference between the moment of inertia, I_{zz}, and the average of the equatorial moments, $(I_{xx}+I_{yy})/2$. Again, since $v_{2,0}<0$, the Earth bulges more around the equator and is flattened at the poles. The second zonal harmonic coefficient is roughly 1000 times larger than the other second-degree coefficients and thus indicates a substantial polar flattening (owing to the Earth's early more fluid state). This flattening is approximately 0.003.

3.02.5.2 Normal Ellipsoidal Field

Because of Earth's dominant polar flattening and the near symmetry of the equator, any meridional section of the Earth

is closer to an ellipse than a circle. For this reason, spheroidal coordinates (eqn [2]) have often been advocated in place of the usual spherical coordinates. In fact, for geodetic positioning and geographic mapping, because of this flattening, the conventional (geodetic) latitude and longitude define the direction of the perpendicular to an ellipsoid, rather than the radial direction from the origin. These geodetic coordinates, however, are not the spheroidal (ellipsoidal) coordinates defined in Section 3.02.1 and would be rather useless in potential modeling because they do not separate Laplace's differential equation.

Solutions to Laplace's equation in terms of the spheroidal coordinates, (δ,λ,u), are developed easily, analogous to the spherical harmonic series (Section 3.02.4) (Hofmann-Wellenhof and Moritz, 2005). Until recently, they have not been adopted in most geodetic applications perhaps in part because of the nonintuitive nature of the coordinates. On the other hand, it is definitely advantageous to model the normal (or reference) gravity field in terms of these coordinates since it is based on an ellipsoid and the corresponding simplicity of the boundary condition results in closed formulas for the potential. Separating Laplace's equation analogous to its form in spherical coordinates, the solution is obtained by successively solving three ordinary differential equations. Applied to the exterior gravitational potential, V, the solution is given by (cf. eqn [50])

$$V(\delta,\lambda,u)=\sum_{n=0}^{\infty}\sum_{m=-n}^{n}\frac{Q_{n|m|}(iu/E)}{Q_{n|m|}(ib/E)}v_{nm}^{e}\overline{Y}_{nm}(\delta,\lambda) \qquad [117]$$

where E is the linear eccentricity associated with the coordinate system and Q_{nm} is the associated Legendre function of the second kind. The coefficients of the series, v_{nm}^{e}, refer to an ellipsoid of semiminor axis, b; and with the series written in this way, they are all real numbers with the same units as V. An exact relationship between these and the spherical harmonic coefficients, v_{nm}, was given by Hotine (1969) and Jekeli (1988). The computation of the functions, Q_{nm}, was advanced recently by Sebera et al. (2012).

With this formulation of the potential, Dirichlet's BVP is solved for an ellipsoidal boundary using the orthogonality of the spherical harmonics:

$$v_{nm}^{e}=\frac{1}{4\pi}\iint_{\sigma}V(\delta,\lambda,b)\overline{Y}_{nm}(\delta,\lambda)\,\mathrm{d}\sigma \qquad [118]$$

where $\mathrm{d}\sigma=\sin\delta\,\mathrm{d}\delta\,\mathrm{d}\lambda$ and $\sigma=\{(\delta,\lambda)|0\le\delta\le\pi,\ 0\le\lambda\le2\pi\}$. Note that while the limits of integration and the differential element, $\mathrm{d}\sigma$, are the same as for the unit sphere, the boundary values are on the ellipsoid.

The simplicity of the boundary values of the *normal* gravitational potential allows its extension into exterior space to be expressed in closed analytic form. Analogous to the geoid in the actual gravity field, the normal ellipsoid is defined to be a level surface in the normal *gravity* field. In other words, the sum of the normal gravitational potential and the centrifugal potential due to Earth's rotation is a constant on the ellipsoid:

$$V^{e}(\delta,\lambda,b)+\phi(\delta,b)=U_0 \qquad [119]$$

Hence, the normal gravitational potential on the ellipsoid, $V^{e}(\delta,\lambda,b)$, depends only on latitude and is symmetrical with respect to the equator. Consequently, it consists of only even zonal harmonics, and because the centrifugal potential has only zero- and second-degree zonals, the corresponding ellipsoidal series is finite (up to degree two). The solution to this Dirichlet problem is given in spheroidal coordinates by

$$V^{e}(\delta,\lambda,u)=\frac{GM}{E}\tan^{-1}\frac{E}{u}+\frac{1}{2}\omega_{e}^{2}a^{2}\frac{q}{q_0}\left(\cos^{2}\delta-\frac{1}{3}\right) \qquad [120]$$

where a is the semimajor axis of the ellipsoid, ω_e is Earth's rate of rotation, and

$$q=\frac{1}{2}\left(\left(1+3\frac{u^2}{E^2}\right)\tan^{-1}\frac{E}{u}-3\frac{u}{E}\right),\quad q_0=q|_{u=b} \qquad [121]$$

Heiskanen and Moritz (1967) and Hofmann-Wellenhof and Moritz (2005) provided details of the straightforward derivation of these and the following expressions.

The equivalent form of V^{e} in spherical harmonics is given by

$$V^{e}(\theta,\lambda,r)=\frac{GM}{r}\left(1-\sum_{n=1}^{\infty}J_{2n}\left(\frac{a}{r}\right)^{2n}P_{2n}(\cos\theta)\right) \qquad [122]$$

where

$$J_{2n}=(-1)^{n+1}\frac{3e^{2n}}{(2n+1)(2n+3)}\left(1-n+\frac{5n}{e^2}J_2\right),\quad n\ge1 \qquad [123]$$

and $e=E/a$ is the first eccentricity of the ellipsoid. The second zonal coefficient is given by

$$J_2=\frac{e^2}{3}\left(1-\frac{2}{15q_0}\frac{\omega_e^2a^2E}{GM}\right)=\frac{I_{zz}^{e}-I_{xx}^{e}}{Ma^2} \qquad [124]$$

where the second equality comes directly from the last of eqn [112] and the ellipsoid's rotational symmetry ($I_{xx}^{e}=I_{yy}^{e}$). This equation also provides a direct relationship between the geometry (the eccentricity or flattening) and the mass distribution (difference of second-order moments) of the ellipsoid. Therefore, J_2 is also known as the dynamic form factor – the flattening of the ellipsoid can be described either geometrically or dynamically in terms of a difference in density moments.

The normal gravitational potential depends solely on four adopted parameters: Earth's rotation rate, ω_e; the size and shape of the normal ellipsoid, for example, a and J_2; and a potential scale, for example, GM. The mean Earth ellipsoid is the normal ellipsoid with parameters closest to actual corresponding parameters for the Earth. GM and J_2 are determined by observing satellite orbits, a can be calculated by fitting the ellipsoid to mean sea level using satellite altimetry, and Earth's rotation rate comes from astronomical observations. Table 2 gives present values and adopted constants for the Geodetic Reference Systems of 1967 and 1980 (GRS67 and GRS80) and the World Geodetic System 1984 (WGS84).

In modeling the disturbing potential in terms of spherical harmonics, one naturally uses the form of the normal gravitational potential given by eqn [122]. Here, we have assumed that all harmonic coefficients refer to a sphere of radius, a. Corresponding coefficients for the series of $T=V-V^{e}$ are, therefore,

Table 2 Defining parameters for normal ellipsoids of geodetic reference systems

Reference system	a *(m)*	J_2	GM *($m^3\ s^{-2}$)*	ω_e *(rad s^{-2})*
GRS67	6378160	1.0827E−3	3.98603E14	7.2921151467E−5
GRS80	6378137	1.08263E−3	3.986005E14	7.292115E−5
WGS84	6378137	1.08262982131E−3	3.986004418E14	7.2921151467E−5
Current IERS values[a]	6378136.6 ± 0.1 (mean–tide system)	(1.0826359 ± 0.0000001) E−03 (zero-tide system)	(3.986004418 ± 0.000000008)E14 (includes atmosphere)	7.292115E−5 (mean value)

[a]Adapted by the International Earth Rotation and Reference System Service (IERS, Petit and Luzum, 2010).

$$\delta C_{nm}^{(a)} = \begin{cases} 0, & n = 0 \\ C_{n0}^{(a)} - \dfrac{-J_n}{\sqrt{2n+1}}, & n = 2, 4, 6, \ldots \\ C_{nm}^{(a)}, & \text{otherwise} \end{cases} \qquad [125]$$

For coefficients referring to the sphere of radius, R, as in eqn [65], we have $\delta C_{nm} = (a/R)^n \delta C_{nm}^{(a)}$. The harmonic coefficients, J_{2n}, attenuate rapidly due to the factor, e^{2n}; and only harmonics up to degree ten are significant.

Normal gravity, being the gradient of the normal gravity potential, is used typically only in applications tied to an Earth-fixed coordinate system. Exact formulas for all its components on and above the ellipsoid may be found in the WGS84 document (NIMA, 2000). For points on the ellipsoid, the only nonzero component is along the ellipsoid normal and is given by the Somigliana formula:

$$\gamma(\phi) = \gamma_a \frac{1 + \left(\frac{b\gamma_b}{a\gamma_a} - 1\right) \sin^2\phi}{\sqrt{1 - e^2 \sin^2\phi}} \qquad [126]$$

where ϕ is geodetic latitude, a, b are the semimajor and semiminor axes of the ellipsoid, and γ_a, γ_b are the values of normal gravity, respectively, at the equator and pole of the ellipsoid. The values of the latter (and b) are constants derived exactly from the four fundamental constants of the normal ellipsoid (Moritz, 2000).

3.02.6 Methods of Determination

In this section, we briefly explore the basic technologies that yield measurements of the gravitational field. Even though we have reduced the problem of determining the exterior potential from a volume integral to a surface integral (e.g., either eqn [72] or [75]), it is clear that in theory, we can never determine the entire field from a finite number of measurements. The integrals will always need to be approximated numerically, and/or the infinite series of spherical harmonics needs to be truncated. However, with enough effort and within the limits of computational capabilities, one can approach the ideal continuum of boundary values as closely as desired or make the number of coefficients in the series representation as large as possible. The expended computational and measurement efforts have to be balanced with the ability to account for inherent model errors (such as the spherical approximation) and the noise of the measuring device. To be useful for geodetic and geodynamic purposes, the instruments must possess a sensitivity of at least a few parts per million, and, in fact, many have a sensitivity of parts per billion. These sensitivities often come at the expense of prolonging the measurements (integration time) in order to average out random noise, thus reducing the achievable temporal resolution. This is particularly critical for moving-base instrumentation such as on an aircraft or satellites where temporal resolution translates into spatial resolution through the velocity of the vehicle.

3.02.6.1 Measurement Systems and Techniques

Determining the gravitational field through classical measurements relies on three fundamental laws. The first two are Newton's second law of motion and his law of gravitation. Newton's law of motion states that the rate of change of linear momentum of a particle is equal to the totality of forces, $\boldsymbol{F}$, acting on it. Given more familiarly as $m_i \mathrm{d}^2\boldsymbol{x}/\mathrm{d}t^2 = \boldsymbol{F}$, it involves the inertial mass, m_i; and, conceptually, the forces, $\boldsymbol{F}$, should be interpreted as action forces, like propulsion or friction. The gravitational field, which is part of the space we occupy, is due to the presence of masses like the Earth, sun, moon, and planets and induces a different kind of force, the gravitational force (Section 3.02.2). It is related to gravitational acceleration, $\boldsymbol{g}$, through the gravitational mass, m_g, according to the law of gravitation, abbreviated here as $m_g\boldsymbol{g} = \boldsymbol{F}_g$. Newton's law of motion must be modified to include $\boldsymbol{F}_g$ separately. Through the third fundamental law, Einstein's equivalence principle, which states that inertial and gravitational masses are indistinguishable, we finally get

$$\frac{\mathrm{d}^2\boldsymbol{x}}{\mathrm{d}t^2} = \boldsymbol{a} + \boldsymbol{g} \qquad [127]$$

where $\boldsymbol{a}$ is the specific force ($\boldsymbol{F}/m_i$), or also the inertial acceleration, due to action forces. This equation holds in a nonrotating, freely falling frame (i.e., an inertial frame), and variants of it can be derived in more complicated frames that rotate or have their own dynamic motion. However, one can always assume the existence of an inertial frame and proceed on that basis.

There exist a variety of devices that measure the motion of an inertial mass with respect to the frame of the device, and thus, technically, they sense $\boldsymbol{a}$; such devices are called accelerometers. Consider the special case that an accelerometer is resting on the Earth's surface with its sensitive axis aligned along the vertical. In an Earth-centered frame (inertial, if we ignore Earth's rotation), the free-fall motion of the accelerometer is impeded by the reaction force of the Earth's surface acting on the accelerometer. In this case, the left side of eqn [127] applied to the motion of the accelerometer is zero,

and the accelerometer, sensing the reaction force, indirectly measures (the negative of) gravitational acceleration. This accelerometer is given the special name, gravimeter.

Gravimeters, especially static instruments, are designed to measure acceleration at very low temporal frequencies (i.e., averaged over longer periods of time), whereas accelerometers, typically used in navigation or other motion-sensing applications, require a much shorter response in order to sense the rapidly changing accelerations. As such, gravimeters generally are more accurate. Earth-fixed gravimeters actually measure gravity (**Section 3.02.1.3**), the combination of gravitation and centrifugal acceleration due to Earth's spin (the frame is not inertial in this case). The simplest, though not the first invented, gravimeter utilizes a vertically, freely falling mass, measuring the time it takes to fall a given distance. Applying eqn [127] to the falling mass in the frame of the device, one can solve for g (assuming it is constant): $x(t) = 0.5gt^2$. Equations can also be developed that account for the linear gradient of gravity. This free-fall gravimeter is a special case of a more general gravimeter that constrains the fall using an attached spring or the arm of a pendulum, where other (action) forces (the tension in the arm or the spring) thus enter into the equation.

The first gravimeter, in fact, was the pendulum, systematically used for gravimetry as early as the 1730s and 1740s by P. Bouguer on a geodetic expedition to measure the size and shape of the Earth (meridian arc measurement in Peru). The pendulum served well into the twentieth century (until the early 1970s) both as an absolute device, measuring the total gravity at a point, and as a relative device indicating the difference in gravity between two points (Torge, 1989). Today, absolute gravimeters exclusively rely on a freely falling mass, where exquisitely accurate measurements of distance and time are achieved with laser interferometers and atomic clocks (Niebauer et al., 1995; Zumberge et al., 1982). Accurate *relative* gravimeters are much less expensive, requiring a measurement of distance change only, and because many errors that cancel between measurements need not be addressed. They rely almost exclusively on a spring-suspended test mass (Nettleton, 1976; Torge, 1989). Developed early in the twentieth century in response to oil exploration requirements, the basic principles of the relative gravimeter have changed little since then. Modern instruments include electronic recording capability and specialized stabilization and damping for deployment on moving vehicles such as ships and aircraft. The accuracy of absolute gravimeters is typically of the order of parts per billion, and relative devices in field deployments may be as good but more typically are at least one order of magnitude less precise. Laboratory relative (in time) gravimeters, based on cryogenic instruments that monitor the virtual motion of a test mass that is electromagnetically suspended using superconducting persistent currents (Goodkind, 1999), are as accurate as portable absolute devices (or more), owing to the stability of the currents and the controlled laboratory environment.

On a moving vehicle, particularly an aircraft, the relative gravitational acceleration can be determined only from a combination of gravimeter and kinematic positioning system. The latter is needed to derive the (vertical) kinematic acceleration (the left side of eqn [127]). Today, the GPS best serves that function, yielding centimeter-level precision in relative three-dimensional position. Such combined GPS/gravimeter systems have been used successfully to determine the vertical component of gravitation over large otherwise inaccessible areas such as the Arctic Ocean (Kenyon and Forsberg, 2000), as well as in regions where conventional surface gravimetry would be much less economical for geoid determination and oil exploration purposes (Gumert, 1998; Hammer, 1983; Olesen and Forsberg, 2007). The airborne gravimeter is specially designed to damp out high-frequency noise and usually is stabilized on a level platform.

Three-dimensional moving-base gravimetry has also been demonstrated using the triad of accelerometers of a high-accuracy inertial navigation system (the type that are fixed to the aircraft without special stabilizing platforms). The orientation of all accelerometers on the vehicle must be known with respect to inertial space, which is accomplished with precision gyroscopes. Again, the total acceleration vector of the vehicle, $\mathrm{d}^2\boldsymbol{x}/\mathrm{d}t^2$, can be ascertained by time differentiation of the kinematic positions (from GPS). One of the most critical errors is due to the cross coupling of the horizontal orientation error, $\delta\psi$, with the large vertical acceleration (the lift of the aircraft, essentially equal to $-g$). This is a first-order effect ($g \sin \delta\psi$) in the estimation of the horizontal gravitation components but only a second-order effect ($g(1-\cos\delta\psi)$) on the vertical component. Details of moving-base vector gravimetry may be found in Jekeli (2000a, **Chapter 1.11**), Kwon and Jekeli (2001), and also Studinger et al. (2008). Further developments and examples of geophysical applications may be found in Lane (2004, 2010).

The ultimate global gravimeter is the satellite in free fall (i.e., in orbit due to sufficient forward velocity) – the satellite is the inertial mass and the 'device' is a set of reference points with known coordinates, for example, on the Earth's surface, or another satellite whose orbit is known. The measuring technology is an accurate ranging system (radar or laser) that tracks the satellite as it orbits (falls to) the Earth. Ever since Sputnik, the first artificial satellite launched into Earth orbit in 1957, Earth's gravitational field could be determined by tracking satellites from precisely known ground stations. Equation [127], with gravitational acceleration expressed as a truncated series of spherical harmonics (gradient of eqn [50]), becomes

$$\frac{\mathrm{d}^2\boldsymbol{x}}{\mathrm{d}t^2} = \sum_{n=0}^{n_{\max}} \sum_{m=-n}^{n} \nu_{nm} \nabla \left(\left(\frac{R}{r} \right)^{n+1} \Upsilon_{nm}(\theta < \lambda + \omega_e t) \right) + \delta\boldsymbol{R} \quad [128]$$

where ω_e is Earth's rate of rotation and $\delta\boldsymbol{R}$ represents residual accelerations due to action forces (solar radiation pressure, atmospheric drag, Earth's albedo, etc.), gravitational tidal accelerations due to other bodies (moon, sun, and planets), and all other subsequent indirect effects. The position vector on the left side of eqn [128] is more explicitly $\boldsymbol{x}(t) = \boldsymbol{x}(\theta(t), \lambda(t) + \omega_e t, r(t))$; and the spatial coordinates on the right side are also functions of time. This makes the equation more conceptual than practical since it is numerically more convenient to transform the satellite position and velocity into Keplerian orbital elements (semimajor axis of the orbital ellipse, its eccentricity, its inclination to the equator, the angle of perigee, the right ascension of the node of the orbit, and the mean motion), all of which also change in time, but most much

more slowly. This transformation was derived by Kaula (1966); see also Seeber (1993).

In the most general case ($n_{\max} > 2$ and $\delta \boldsymbol{R} \neq 0$), there is no analytic solution to eqn [128] or to its transformations to other types of coordinates. The positions of the satellite are observed by ranging techniques, and the unknowns to be solved are the coefficients, v_{nm}. Numerical integration algorithms have been specifically adapted to this problem, and extremely sophisticated models for $\delta \boldsymbol{R}$ are employed with additional unknown parameters to be solved in order to estimate as accurately as possible the gravitational coefficients (e.g., Cappelari et al., 1976; Pavlis et al., 1999). The entire procedure falls under the broad category of dynamic orbit determination, and the corresponding gravitational field modeling may be classified as the *time-wise* approach. The partial derivatives of eqn [128] with respect to unknown parameters, $\boldsymbol{p} = \{\ldots, v_{nm}, \ldots\}$, termed the *variational equations*, are integrated numerically in time, yielding estimates for $H = \partial \boldsymbol{x}/\partial \boldsymbol{p} = \{\ldots, \partial \boldsymbol{x}/\partial v_{nm}, \ldots\}$. These are then used in a least-squares adjustment of the linearized model relating observed positions (e.g., via ranges) to parameters:

$$\delta \boldsymbol{x} = H \delta \boldsymbol{p} + \varepsilon \qquad [129]$$

where $\delta \boldsymbol{x}$ and $\delta \boldsymbol{p}$ are differences with respect to previous estimates and $\boldsymbol{\varepsilon}$ represents errors (Tapley, 1973).

The alternative to this rather complicated estimation of the gravitational field by tracking satellites is the *in situ* measurement of the field. However, a gravimeter (or accelerometer) on a satellite does not sense the presence of a gravitational field. This is evident from the fact that the satellite is in free fall (apart from small accelerations due to action forces such as atmospheric drag) and the inertial test mass and the gravimeter, itself, are equally affected by gravitation (i.e., they are all in free fall). On the other hand, two accelerometers fixed on a satellite yield, through the difference in their outputs, a gradient in acceleration that includes the gradient of gravitation. On a nonrotating satellite, the acceleration at an arbitrary point, $\boldsymbol{b}$, of the satellite is given by

$$\boldsymbol{a}_b = \frac{\mathrm{d}^2 \boldsymbol{x}}{\mathrm{d}t^2} - \boldsymbol{g}(\boldsymbol{b}) \qquad [130]$$

in a coordinate system with origin at the center of mass of the satellite. Taking the difference (differential) of two accelerations in ratio to their separation, $\delta \boldsymbol{b}$, we obtain

$$\frac{\delta \boldsymbol{a}_b}{\delta \boldsymbol{b}} = -\frac{\delta \boldsymbol{g}}{\delta \boldsymbol{b}} \qquad [131]$$

where the ratios represent tensors of derivatives in the local satellite coordinate frame. That is, the kinematic acceleration of the satellite is the same for both points on the satellite and cancels. For a rotating satellite, this equation generalizes to

$$\frac{\partial \boldsymbol{a}_b}{\partial \boldsymbol{b}} = -\frac{\partial \boldsymbol{g}_b}{\partial \boldsymbol{b}} + \Omega^2 + \frac{\mathrm{d}}{\mathrm{d}t}\Omega \qquad [132]$$

where Ω is a skew-symmetrical matrix whose off-diagonal elements are the components of the vector that defines the rotation rate of the satellite with respect to the inertial frame.

Thus, a *gravitational gradiometer* on a satellite (or any moving vehicle) senses a combination of gravitational gradient and angular acceleration (including a centrifugal type). In principle, if the entire tensor of gradients is measured, then, because of the symmetry of the gravitational gradient tensor and of Ω^2 and the antisymmetry of $\mathrm{d}\Omega/\mathrm{d}t$, the sum $\delta \boldsymbol{a}_b/\delta \boldsymbol{b} + (\delta \boldsymbol{a}_b/\delta \boldsymbol{b})^{\mathrm{T}}$ eliminates the latter, while the difference $\delta \boldsymbol{a}_b/\delta \boldsymbol{b} - (\delta \boldsymbol{a}_b/\delta \boldsymbol{b})^{\mathrm{T}}$ can be used to infer Ω, subject to initial conditions.

When the two ends of the gradiometer are fixed to one frame, the common linear acceleration, $\mathrm{d}^2\boldsymbol{x}/\mathrm{d}t^2$, cancels, as shown earlier; but if the two ends are independent, disconnected platforms moving in similar orbits, the gravitational difference depends also on their relative motion in inertial space. This is the concept for satellite-to-satellite tracking, by which one satellite precisely tracks the other and the change in the range rate between them is the consequence of a combination of gravitational difference, a difference in action forces, and a centrifugal acceleration due to the rotation of the baseline of the satellite pair. It can be shown that the line-of-sight acceleration (the measurement) is given by

$$\frac{\mathrm{d}^2 \rho}{\mathrm{d}t^2} = \boldsymbol{e}_\rho^{\mathrm{T}}(\boldsymbol{g}(\mathrm{x}_2) - \boldsymbol{g}(\mathrm{x}_1)) + \boldsymbol{e}_\rho^{\mathrm{T}}(\boldsymbol{a}_2 - \boldsymbol{a}_1) + \frac{1}{\rho}\left(\left|\frac{\mathrm{d}}{\mathrm{d}t}\Delta \mathrm{x}\right|^2 - \left(\frac{\mathrm{d}\rho}{\mathrm{d}t}\right)^2\right) \qquad [133]$$

where $\boldsymbol{e}_\rho$ is the unit vector along the instantaneous baseline connecting the two satellites, ρ is the baseline length (the range), and $\Delta \boldsymbol{x} = \boldsymbol{x}_2 - \boldsymbol{x}_1$ is the difference in position vectors of the two satellites. Clearly, only the gravitational difference projected along the baseline can be determined (similar to a single-axis gradiometer) and then only if both satellites carry accelerometers that sense the nongravitational accelerations. Also, the orbits of both satellites must be known in order to account for the last (centrifugal) term.

An Earth-orbiting satellite clearly is the ideal platform on which to measure the gravitational field when seeking global coverage in relatively short time. One simply designs the orbit to be polar and circular; and as the satellite orbits, the Earth spins underneath, offering a different section of its surface on each satellite revolution. There are also limitations. The satellite must have low altitude, h, above the Earth's sphere of radius, R, in order to achieve high sensitivity, since the nth-degree harmonics of the field attenuate as $(R/(R+h))^{n+1}$. On the other hand, the lower the altitude, the shorter is the life of the satellite due to atmospheric drag, which can only be countered with onboard propulsion systems. Secondly, because of the inherent speed of lower-orbit satellites (about 7 km s^{-1}), the resolution of its measurements is limited by the integration (averaging) time of the sensor (typically 1–10 s). Higher resolution comes only with shorter integration time, which may reduce the accuracy if this depends on averaging out random noise. Figure 9 shows the corresponding achievable resolution on the Earth's surface for different satellite instrumentation parameters, length of time in polar orbit and along-orbit integration time, or smoothing (Jekeli, 2004). In each case, the indicated level of resolution is warranted only if the noise of the sensor (after smoothing) does not overpower the signal at this resolution.

Being a higher-order derivative of the gravitational potential, gravitational gradients are particularly revealing of sharp contrasts in Earth's mass density structure. And although the gravitational gradients attenuate away from a source body with one additional power of distance (compared to gravitational

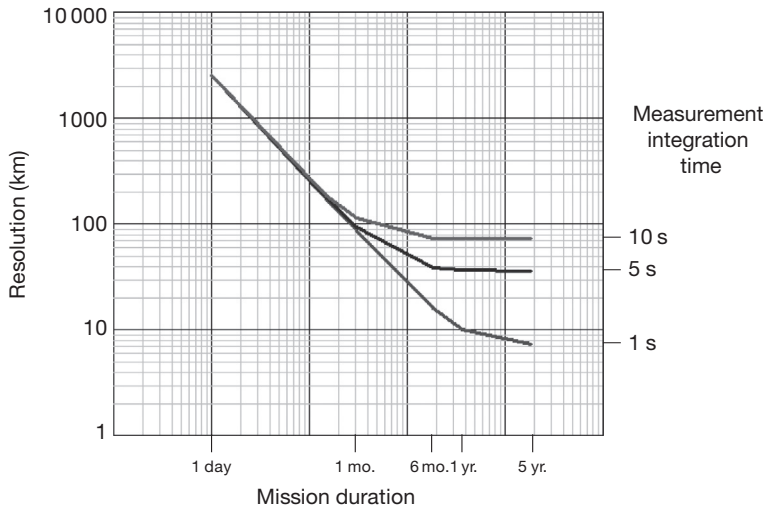

Figure 9 Spatial resolution of satellite measurements versus mission duration and integration time. The satellite altitude is 450 km. Reproduced from Jekeli C (2004) High-resolution gravity mapping: the next generation of sensors. In: Sparks RSJ (ed.) The State of the Planet: Frontiers and Challenges in Geophysics, Geophysical Monograph 150, IUGG, vol. 19, pp. 135–146, with permission from American Geophysical Union.

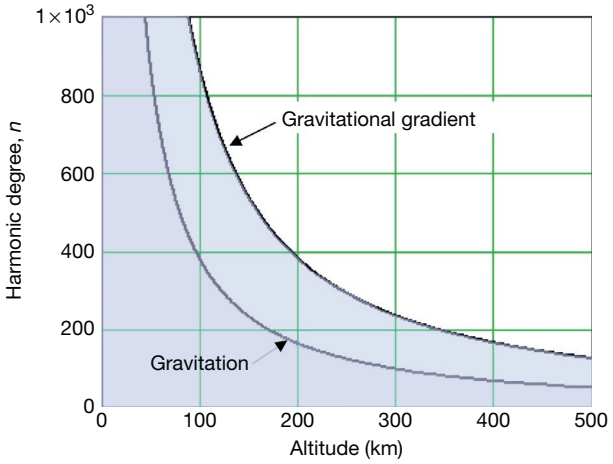

Figure 10 The product, $n^q(R/(R+h))^{n+1+q}$, of derivative and upward continuation frequency responses as a function of altitude, h, and harmonic degree, n, for gravitation ($q=1$) and its gradient ($q=2$). The shaded area represents the domain in each case where this product is greater than unity and thus does not attenuate the field.

acceleration), this is more than compensated by the increased sensitivity to (shorter) wavelengths. Indeed, the geopotential field spectrum scales by $\sim n^q$ due to q radial derivatives of the field, while it scales by $(R/(R+h))^{n+1+q}$ due to upward continuation. When the combination of these effects is greater than unity, there is no physical attenuation in the corresponding spectral component. As seen in Figure 10, for all altitudes, the recoverable spectrum generally is always greater with gravity gradiometry ($q=2$) than with gravimetry ($q=1$). Thus, for optimal resolution, *in situ* gravity gradiometry is preferred on satellite missions.

Two satellite-to-satellite tracking systems were launched to determine the global gravitational field. One is CHAMP (Challenging Minisatellite Payload) in 2000 (Reigber et al., 2002) and the other is GRACE (Gravity Recovery and Climate Experiment) in 2002 (Tapley et al., 2004a). CHAMP is a single low-orbiting satellite (400–450 km altitude) being tracked by the high-altitude GPS satellites, and it also carries a magnetometer to map the Earth's magnetic field. GRACE is more specifically dedicated to determining with extremely high accuracy the long to medium wavelengths of the gravitational field and their temporal variations. With two satellites in virtually identical low Earth orbits, one following the other, the primary GRACE data consist of intersatellite ranges observed by K/Ka-band radar with 10 μm precision in the 10 Hz bandwidth. The objective is to sense changes in the gravitational field due to mass transfer on the Earth within and among the atmosphere, the hydrosphere/cryosphere, and the oceans (Tapley et al., 2004b).

A gravity gradiometer was launched for the first time in March 2009 with the satellite GOCE (Gravity Field and Steady-State Ocean Circulation Explorer; Rummel et al., 2002, 2011) whose mission is dedicated to modeling the static Earth's gravitational field to high resolution (maximum harmonic degree, 250). The GOCE gradiometer consists of three pairs of three-degree-of-freedom accelerometers that sense all nine gradient tensor elements, although only the diagonal and a third of the off-diagonal elements achieve the highest performance due to limitations in calibration. The spectral band of the measurements is 0.005–0.1 Hz and the noise floor is about $10-20\times10^{-12}\ \mathrm{s}^{-2}/\sqrt{\mathrm{Hz}}$.

Both CHAMP and GRACE have yielded global gravitational models by utilizing traditional satellite tracking methods and incorporating the range rate appropriately as a tracking observation (time-wise approach). However, the immediate application of eqn [133] suggests that gravitational differences can be determined *in situ* and used to determine a model for the global field directly. This is classified as the space-wise approach. In fact, if the orbits are known with sufficient accuracy (from kinematic orbit determination, e.g., by GPS), this procedure utilizes a linear relationship between observations and unknown harmonic coefficients:

$$\left.\frac{\mathrm{d}^2\rho}{\mathrm{d}t^2}\right|_{x_1,x_2} = \sum_{n=0}^{n_{\max}}\sum_{m=-n}^{n} v_{nm}\boldsymbol{e}_\rho^{\mathrm{T}}\left(\boldsymbol{\nabla}U_{nm}(\theta,\lambda,r)|_{x_2} - \boldsymbol{\nabla}U_{nm}(\theta,\lambda,r)|_{x_1}\right) + \delta a + \delta c \qquad [134]$$

where $U_{nm}(\theta,\lambda,r) = (R/r)^{n+1}\overline{Y}_{nm}(\theta,\lambda)$ and δa and δc are the last two terms in eqn [133]. Given the latter and a set of line-of-sight accelerations, a theoretically straightforward linear least-squares adjustment solves for the coefficients. A similar procedure can be used for gradients observed on an orbiting satellite, such as GOCE:

$$\left.\frac{\partial \boldsymbol{a}}{\partial \boldsymbol{b}}\right|_{\boldsymbol{x}} = \sum_{n=0}^{n_{\max}}\sum_{m=-n}^{n} v_{nm}\boldsymbol{\nabla}\boldsymbol{\nabla}^{\mathrm{T}}U_{nm}(\theta,\lambda,r)|_{x} + \boldsymbol{\psi} \qquad [135]$$

where $\boldsymbol{\psi}$ comprises the rotational acceleration terms in eqn [132].

Recently, a rather different theory has been considered by several investigators to model the gravitational field from satellite-to-satellite tracking observations. The method, first proposed by Wolff (1969), makes use of yet another fundamental law: the law of conservation of energy. Simply, the range rate between two satellites implies an along-track velocity difference or a difference in kinetic energy. Observing this difference leads directly, by the conservation law, to the difference in potential energy, that is, the gravitational potential and other potential energies associated with action forces and Earth's rotation. Neglecting the latter two, conservation of energy implies

$$V = \frac{1}{2}\left|\frac{\mathrm{d}}{\mathrm{d}t}\boldsymbol{x}_1\right|^2 - E_0 \qquad [136]$$

where E_0 is a constant. Taking the along-track differential, we have approximately

$$V(\boldsymbol{x}_2) - V(\boldsymbol{x}_1) \approx \delta V = \left|\frac{\mathrm{d}}{\mathrm{d}t}\boldsymbol{x}_1\right| \frac{\mathrm{d}}{\mathrm{d}t}\rho \qquad [137]$$

where $|\delta(\mathrm{d}\boldsymbol{x}_1/\mathrm{d}t)| \approx |\mathrm{d}\boldsymbol{x}_2/\mathrm{d}t - \mathrm{d}\boldsymbol{x}_1/\mathrm{d}t| \approx \mathrm{d}\rho/\mathrm{d}t$. This very rough conceptual relationship between the potential difference and the range rate applies to two satellites closely following each other in similar orbits. The precise formulation is given by Jekeli (1999) and holds for any pair of satellites, not just two low orbiters. Mapping range rates between two polar orbiting satellites (such as GRACE) yields a global distribution of potential difference observations related again linearly to a set of harmonic coefficients:

$$V(\boldsymbol{x}_2) - V(\boldsymbol{x}_1) = \sum_{n=0}^{n_{\max}}\sum_{m=-n}^{n} v_{nm}\left(U_{nm}(\theta,\lambda,r)|_{x_2} - U_{nm}(\theta,\lambda,r)|_{x_1}\right) \qquad [138]$$

The energy-based model holds for any two vehicles in motion and equipped with the appropriate ranging and accelerometry instrumentation. For example, the energy conservation principle could also be used to determine geopotential differences between an aircraft and a satellite, such as a GPS satellite (at which location the geopotential is known quite well). The aircraft would require only a GPS receiver (to do the ranging) and a set of accelerometers (and gyros for orientation) to measure the action forces (the same system components as in airborne accelerometry discussed earlier). Resulting potential differences could be used directly to model the geoid undulation differences using Bruns' equation [3].

The *in situ* measurements of line-of-site acceleration or of more local gradients would need to be reduced from the satellite orbit to a well-defined surface (such as a sphere) in order to serve as boundary values in a solution to a BVP. However, the model for the field is already in place, rooted in potential theory (truncated series solution to Laplace's equation), and one may think of the problem more in terms of fitting a three-dimensional model to a discrete set of observations. This operational approach can readily, at least conceptually, be expanded to include observations from many different satellite systems, even airborne and ground-based observations.

3.02.6.2 Models

Global spherical harmonic models have been derived since the first satellite launches in the 1960s using a variety of methods and combinations of terrestrial data and satellite tracking and *in situ* data. The recent gravity satellite missions have generated a plethora of such models, which are collected and organized by the International Center for Earth Gravitational Models (ICEGM (http://icgem.gfz-potsdam.de/ICGEM/)) of the International Association of Geodesy (IAG). The spherical harmonic models come in two varieties, either based strictly on satellite data, in which case, their resolution is limited as discussed earlier or combined with terrestrial data, including satellite altimetry over the oceans, for vastly higher resolution. The responsible centers for collecting, distributing, and archiving the raw satellite data make these (satellite) data and the derived global models available for general scientific investigations.

The standard solution to the BVP (**Section 3.02.4**), using terrestrial gravimetry in the form of gravity anomalies, now routinely incorporates a longer-wavelength global model derived from satellite data (such as GRACE or GOCE). The solution is either regional using Green's function approach, Stokes' integral (eqn [72]), or global, based on the harmonic analysis of surface data, either using the integrals [75] or solving a linear system of equations (eqn [71] truncated to finite degree) to obtain the higher-degree coefficients, δC_{nm}. The integrals must be evaluated using quadratures, and very fast numerical techniques have been developed when the data occupy a regular grid of coordinates on the sphere or ellipsoid (Rapp and Pavlis, 1990). Similar algorithms enable the fast solution of the linear system of eqn [71].

For the global harmonic analysis, the number of coefficients, $(n_{\max}+1)^2$, must not be greater than implied by the resolution of the data. A general, conservative rule of thumb for the relationship between the maximum resolution (half-wavelength), $\Delta\theta$, in angular degrees on the unit sphere, and the maximum degree of a truncated spherical harmonic series is

$$\Delta\theta = \frac{180^\circ}{n_{\max}} \qquad [139]$$

Thus, data on a $1\times1^\circ$ angular grid of latitudes and longitudes would imply $n_{\max}=180$. The number of data (64 800, in this

case) is amply larger than the number of coefficients (32761). This majority suggests a least-squares adjustment of the coefficients to the data, in either method, especially because the data have errors (Rapp, 1969). As $n_{\max}$ increases, a rigorous, optimal adjustment usually is feasible, for a given computational capability, only under restrictive assumptions on the correlations among the errors in the data. Also, the obvious should be noted that the accuracy of the global model in any area depends on the quality of the data in that area. Furthermore, considering that a measurement implicitly contains all harmonics (up to the level of measurement error), the estimation of a finite number of harmonics from boundary data on a given grid is corrupted by those harmonics that are in the data but are not specifically estimated. This phenomenon is called aliasing in spectral analysis and can be mitigated by appropriate filtering of the data (Jekeli, 1996).

The currently best known and arguably the overall most accurate model is EGM08 (Earth Gravitational Model 2008) complete to degree and order $n_{\max}=2160$ (5′ resolution) with additional higher-degree harmonics up to 2190 (Pavlis et al., 2012). This model updates the previous EGM96 (Lemoine et al., 1998) for the WGS84 of the US Department of Defense by including improved gravity anomalies over the oceans derived from satellite altimetry, additional land data sets, and airborne gravimetry and the GRACE gravitational field model to maximum degree and order, $n_{\max}=180$. This latter model was used with its formal covariance error measure and replaced the previously used satellite tracking data that defined the lower-degree harmonics of EGM96. In constructing combination solutions of this type, great effort is expended to ensure the proper weighting of all observations in order to extract the most appropriate information from the diverse data, pertaining to different parts of the spatial gravitational spectrum. It is beyond the present scope to delve into the detailed numerical methodology of combination methods; useful starting points are the documents for EGM96 and EGM08, cited earlier.

Stokes' integral is used in practice today only to take advantage of local or regional data with higher resolution than available from the global models. Even though the integral is a global integral, it can be truncated to a neighborhood of the computation point since Stokes' kernel attenuates rapidly with distance from its origin. Moreover, the corresponding truncation error may be reduced if the boundary values exclude the longer-wavelength features of the field. The latter constitute an adequate representation of the remote zone contribution and can be included separately as follows. Let $\Delta g^{(n_{\max})}$ denote the gravity anomaly implied by a spherical harmonic model, such as given by eqn [71], truncated to degree, $n_{\max}$. From the orthogonality of spherical harmonics (eqn [52]), it is easy to show that

$$\begin{aligned} T^{(n_{\max})}(\theta,\lambda,r) &= \frac{GM}{R}\sum_{n=2}^{n_{\max}}\sum_{m=-n}^{n}\left(\frac{R}{r}\right)^{n+1}\delta C_{nm}\overline{Y}_{nm}(\theta,\lambda) \\ &= \frac{R}{4\pi}\iint_{\sigma}\Delta g^{(n_{\max})}\left(\theta',\lambda',R\right)S(\psi,r)\,\mathrm{d}\sigma \end{aligned} \qquad [140]$$

Thus, given a spherical harmonic model $\{\delta C_{nm}|\ 2\le n\le n_{\max},\ -n\le m\le n\}$, one first removes the model in terms of the gravity anomaly and then restores it in terms of the disturbing potential, changing Stokes' formula [72] to

$$\begin{aligned} T(\theta,\lambda,r) = \frac{R}{4\pi}\iint_{\sigma}\left(\Delta g\left(\theta',\lambda',R\right)-\Delta g^{(n_{\max})}\left(\theta',\lambda',R\right)\right)S(\psi,r)\,\mathrm{d}\sigma \\ + T^{(n_{\max})}(\theta,\lambda,r) \end{aligned} \qquad [141]$$

In theory, if $\Delta g^{(n_{\max})}$ has no errors, then the residual $\Delta g-\Delta g^{(n_{\max})}$ excludes all harmonics of degree $n\le n_{\max}$, and orthogonality would also allow the exclusion of these harmonics from S. Once the integration is limited to a neighborhood of (θ,λ,R), as it must be in practice, there are a number of ways to modify the kernel so as to minimize the resulting truncation error (Sjöberg, 1991, and references therein); for a review, see also Featherstone (2013). The removal and restoration of a global model, however, is the key aspect in all these methods.

In practical applications, the boundary values are on the geoid, being the surface that satisfies the boundary condition of the Robin or Neumann BVP (**Section 3.02.3.2**); that is, we require the normal derivative on the boundary, and measured gravity is indeed the derivative of the potential along the perpendicular to the geoid. The integral in eqn [141] thus approximates the geoid by a sphere. Furthermore, it is assumed that no masses exist external to the geoid. Part of the reduction to the geoid of data measured on the Earth's surface involves redistributing the topographic masses on or below the geoid. This redistribution is undone outside the solution to the BVP (i.e., Stokes' integral) in order to regain the disturbing potential for the actual Earth. Conceptually, we may write

$$T_P=\frac{R}{4\pi}\iint_{\sigma}\left(\Delta g-\Delta g^{(n_{\max})}-\delta c\right)_{P'}S_{P,P'}\ \mathrm{d}\sigma+T_P^{(n_{\max})}+\delta T_P \qquad [142]$$

where δc is the gravity reduction that brings the gravity anomaly to a geoid with no external masses and δT_P is the effect (called indirect effect) on the disturbing potential due to reversing this reduction. This formula holds for T anywhere on or above the geoid and thus can also be used to determine the geoid undulation according to Bruns' formula [3].

3.02.7 The Geoid and Heights

The traditional reference surface, or datum, for heights is the geoid (**Section 3.02.1.3**). A point at mean sea level usually serves as starting point (datum origin), and this defines the datum for vertical control over a region or country. The datum (or regional geoid) is the level continuation of the reference surface under the continents; and the determination of gravity potential differences from the initial point to other points on the Earth's surface, obtained by leveling and gravity measurements, yields heights with respect to that reference (or in that datum). The gravity potential difference, known as the geopotential number, at a point, P, relative to the datum origin, $\overline{P}_0$, is given by (since gravity is the negative vertical derivative of the gravity potential)

$$C_P=W_0-W_P=\int_{\overline{P}_0}^{P}g\,\mathrm{d}n \qquad [143]$$

where g is gravity magnitude, dn is a leveling increment along the vertical direction, and W_0 is the gravity potential at $\overline{P}_0$. By the conservative nature of the gravity potential (eqn [24]), whatever path is taken for the integral yields a unique geopotential number for P. From these potential differences, one can define various types of height, for example, the orthometric height (Figure 3):

$$H_P = \frac{C_P}{\overline{g}_P} \qquad [144]$$

where

$$\overline{g}_P = \frac{1}{H_P}\int_{P_0}^{P} g\,\mathrm{d}H \qquad [145]$$

is the average value of gravity along the plumb line from the geoid at P_0 to P. Other height systems are also in use, such as the normal and dynamic heights:

$$H_P^N = \frac{C_P}{\overline{\gamma}_P}, \quad \overline{\gamma}_P = \frac{1}{H_P^N}\int_{Q_0}^{Q} \gamma\,\mathrm{d}H^N \qquad [146]$$

$$H_P^{\mathrm{dyn}} = \frac{C_P}{\gamma_0}, \quad \gamma_0 = \text{constant} \qquad [147]$$

where reference is made to Hofmann-Wellenhof and Moritz (2005, **Chapter 1.05**), Jekeli (2000b), and NGS (1986) for additional details.

For a particular height datum, there is theoretically only one datum surface (the geoid). But access to this surface is far from straightforward at points other than at the defined datum origin. If $\overline{P}_0$ is defined at mean sea level, other points at mean sea level are not on the same level surface, since mean sea level, in fact, is not level. Erroneously assuming that mean sea level is an equipotential surface can cause significant distortions in the vertical control network of larger regions, as much as several decimeters. This was the case, for example, for the National Geodetic Vertical Datum of 1929 in the United States for which 26 mean sea level points on the East and West Coasts were assumed to lie on the same level surface. Accessibility to the geoid (once defined) at any point is achieved either with precise leveling and gravity, according to eqns [143] and [144], or with precise geometric vertical positioning and knowledge of the gravity potential, as described later in this section. Indeed, as models for the geopotential improve, traditional vertical data may be replaced with a geopotential-based datum that completely eliminates the need for leveling. As noted in **Section 3.02.1**, Canada (in 2013) and the United States (to be implemented in the early 2020s) have embarked on this new paradigm for vertical control.

Geometric vertical positioning, today, is obtained very accurately (cm accuracy or even better) with differential GPS. Suppose that an accurate gravity potential model is also available in the same coordinate system as used for GPS. Then, determining the GPS position at $\overline{P}_0$ allows the evaluation of the gravity potential, W_0, of the datum. From a practical standpoint, one may choose many points near sea level and define an average value of W_0 as the datum or geoid potential. Access to the geoid at any other point, P, or equivalently, determining the orthometric height, H_P, can be done by first determining the ellipsoidal height, h, from GPS. Then, as shown in Figure 3,

$$H_P = h_P - N \qquad [148]$$

where, with $T = W - U$ evaluated on the geoid, Bruns' extended equation (**Section 3.02.1**) yields

$$N = T/\gamma - (W_0 - U_0)/\gamma \qquad [149]$$

where U_0 is the normal gravity potential of the normal ellipsoid. Here, it is noted that models for T (**Section 3.02.6.2**) generally exclude a constant term, which implies that T/γ is the height of a global geoid with respect to a best-fitting ellipsoid. For a predefined ellipsoid (given U_0), and a predefined datum point, $\overline{P}_0$ (or geopotential value, W_0), the second term in eqn [149] is determined independently of the geopotential model.

In a sense, determining N requires N in order to locate the point of computation of T on the geoid. However, only an approximate height, H, suffices to reduce the value of T onto the geoid, where because of the vertical gradient of the order of 5×10^{-4} m s^{-2}, a height error of 20 m leads to an error of 10^{-2}m^2 s^{-2} in T or just 1 mm in the geoid undulation. It should be noted that a model for the disturbing potential as a series of spherical harmonics, for example, derived from satellite observations, satisfies Laplace's equation and, therefore, does not give the correct disturbing potential at the geoid (if it lies below the Earth's surface where Laplace's equation does not hold). Details for the proper evaluation of the geoid undulation from spherical harmonic series of the geopotential are given by Lemoine et al. (1998, **Chapter 1.13**).

The ability to derive orthometric heights (or other geopotential-related heights) from GPS has enormous economical advantage over the alternative and laborious leveling procedure. This has put great emphasis on obtaining an accurate geoid undulation model for land areas. **Section 3.02.6** briefly outlined the essential methods to determine the geopotential from a combination of spherical harmonics and an integral of local gravity anomalies. Bruns' equation then yields the geoid undulation; and as noted earlier, when dealing with a height datum or a regional geoid, the constant $N_0 = -(W_0 - U_0)/\gamma$ requires careful attention (Lemoine et al., 1998, **Chapter 1.13**). It can be determined by comparing the geoid undulation computed according to a model that excludes this term (such as eqn [141]) with at least one geoid undulation (usually many) determined from leveling and GPS, according to eqn [148]; for an example, see Jekeli et al. (2012). Vertical control and the choice of height datum are specific to each country or continent, where a local mean sea level was the adopted datum origin. Thus, height data around the world are 'local geoids' or 'regional geoids' that have significant level differences between them. Investigations and efforts have been under way for many decades to define a global vertical datum; however, an internationally implemented geoid is still in the future, as global geopotential models become more accurate and, perhaps more crucially, as unavoidable differences in mean sea level between conventional datums become secondary to absolute global vertical control. The current convention within the IERS (Petit and Luzum, 2010) is to define the global geoid by the potential value, $W_0 = 62636856.0 \pm 0.5$ m^2 s^{-2}.

On the oceans, the situation is somewhat less complicated. Oceanographers who compute sea surface topography from satellite altimetry on the basis of eqn [148] depend critically

on an accurate geoid undulation or equivalently on an accurate model of T. However, no reduction of the disturbing potential from mean sea level to the geoid is necessary; the deviation between the two being at most 2 m, and if neglected, causes an error in geoid undulation of less than 0.1 mm. Thus, a high-degree spherical harmonic model of T is entirely appropriate. Furthermore, it is reasonable to require that the constant, $W_0 - U_0$, vanishes over the oceans. That is, one may choose the geoid such that it best fits global mean sea level and choose an ellipsoid that best fits this geoid. It means that the global average value of the geoid undulation should be zero (according to eqn [149]). The latter can be achieved with satellite altimetry and oceanographic models of sea surface topography (Bursa et al., 1997).

Several interesting and important distinctions should be made in regard to the tidal effects on the geoid. The sun and the moon generate an appreciable gravitational potential near the Earth (the other planets may be neglected). In an Earth-fixed coordinate system, this extraterrestrial potential varies in time with different periods due to the relative motions of the moon and sun and because of Earth's rotation (Torge and Müller, 2012, p. 88). There is also a constant part, the permanent tidal potential, representing the average over time. It is not zero because the Earth–sun–moon system is approximately coplanar. For each extraterrestrial body with mass, M_B, and distance, r_B, from the Earth's center, this permanent part is given by

$$V_c^B(\theta, r) = \frac{3}{4} G M_B \frac{r^2}{r_B^2} \left(3\cos^2\theta - 1\right)\left(\frac{1}{2}\sin^2\varepsilon - \frac{1}{3}\right) \qquad [150]$$

where ε is the angle of the ecliptic relative to the equator ($\varepsilon \approx 23°44'$). Using nominal parameter values for the sun and the moon, we obtain at mean earth radius, $R = 6371$ km,

$$V_c^{s+m}(\theta, R) = -0.97\left(3\cos^2\theta - 1\right)\mathrm{m}^2\mathrm{s}^{-2} \qquad [151]$$

The gravitational potential from the sun and moon also deforms the quasi-elastic Earth's masses with the same periods and similarly includes a constant part. These mass displacements (both ocean and solid Earth) give rise to an additional indirect change in potential, the tidal deformation potential (there are also secondary indirect effects due to loading of the ocean on the solid Earth, which can be neglected in this discussion). The indirect effect is modeled as a fraction of the direct effect (Lambeck, 1988, p. 254), so that the permanent part of the tidal potential including the indirect effect is given by

$$\overline{V}_c^{s+m}(\theta, R) = (1 + k_2) V_c^{s+m}(\theta, R) \qquad [152]$$

where $k_2 = 0.29$ is Love's number (an empirical number based on observation). This is also called the mean tidal potential.

The mean tidal potential is inherent in all our terrestrial observations (the boundary values) and cannot be averaged away in time; yet, the solutions to the BVP assume no external masses. Therefore, in principle, the effect of the tidal potential including its mean, or permanent, part should be removed from the observations prior to applying the BVP solutions. On the other hand, the permanent indirect effect is not that well modeled and arguably should not be removed; after all, it contributes to the Earth's shape as it actually is in the mean. Three types of tidal systems have been defined to distinguish between these corrections. A *mean* quantity refers to the quantity that retains the mean tidal potential (but time-varying parts are removed); a *nontidal* quantity implies that all tidal effects (time-varying, permanent, direct, and indirect effects) have been removed computationally; and the *zero-tide* quantity excludes all time-varying parts and the permanent direct effect, but it retains the indirect permanent effect.

If the geoid (an equipotential surface) is defined solely by its potential, W_0, then a change in the potential due to the tidal potential, V^{tide} (time-varying and constant parts and direct and indirect effects), implies that the W_0-equipotential surface has been displaced. The geoid is now a different surface with the same W_0. This displacement is equivalent to a change in geoid undulation, $\delta N = V^{\mathrm{tide}}/\gamma$, with respect to some predefined ellipsoid. The permanent tidal effect (direct and indirect) on the geoid is given by

$$\delta\overline{N}(\theta) = -0.099(1 + k_2)\left(3\cos^2\theta - 1\right)\mathrm{m} \qquad [153]$$

If N represents the instantaneous geoid undulation, then the geoid undulation without any tidal effects, that is, the nontidal geoid undulation, is given by

$$N_{\mathrm{nt}} = N - \delta N \qquad [154]$$

The mean geoid undulation is defined as the geoid undulation with all but the mean tidal effects removed:

$$\overline{N} = N - \left(\delta N - \delta\overline{N}\right) \qquad [155]$$

It is the geoid undulation observed, for example, using satellite altimetry, averaged over time (considering only tide-induced variations). We omit here a discussion of secular changes in the geoid due to long-term deformation of the Earth due, in particular, to postglacial isostatic adjustments in the higher north and south latitudes. The zero-tide geoid undulation retains the permanent indirect effect, but no other tidal effects:

$$N_z = N - \left(\delta N + 0.099 k_2\left(3\cos^2\theta - 1\right)\right)\mathrm{m} \qquad [156]$$

The difference between the mean and zero-tide geoids is, therefore, the permanent component of the direct tidal potential. We note that, in principle, each of the geoids defined earlier has the same potential value, W_0, in its own field. That is, with each correction, we define a new gravity field and the corresponding geoid undulation defines the equipotential surface in that field with potential value given by W_0. This is fundamentally different than what happens in the case when the geoid is defined as a vertical datum using a specified datum origin point. In this case, one needs to consider also the vertical displacement of the datum point due to the tidal deformation of the Earth's surface. The potential of the datum then changes because of the direct tidal potential, the indirect effect due to mass changes, and the indirect effect due to the vertical displacement of the datum (for additional details, see Jekeli, 2000b).

References

Bursa M, Radej K, Sima Z, True S, and Vatrt V (1997) Determination of the geopotential scale factor from TOPEX/Poseidon satellite altimetry. *Studia Geophysica et Geodaetica* 41: 203–216.

Cappelari JO, Velez CE, and Fuchs AJ (eds.) (1976) *Mathematical Theory of the Goddard Trajectory Determination System*. Greenbelt, MD: Goddard Space Flight Center, GSFC Document X-582-76-77.

Chao BF (2005) On inversion for mass distribution form global (time-variable) gravity field. *Journal of Geodynamics* 29: 223–230.

Courant R and Hilbert D (1962) *Methods of Mathematical Physics*, vol. 2. New York: Wiley.

Cushing JT (1975) *Applied Analytical Mathematics for Physical Scientists*. New York: Wiley.

Dziewonsky AD and Anderson DL (1981) Preliminary reference Earth model. *Physics of the Earth and Planetary Interiors* 25: 297.

Featherstone WE (2013) Deterministic, stochastic, hybrid and band-limited modifications of Hotine's integral. *Journal of Geodesy* 87(5): 487–500.

Fei ZL and Sideris MG (2000) A new method for computing the ellipsoidal correction for Stokes's formula. *Journal of Geodesy* 74(2): 223–231.

Goodkind JM (1999) The superconducting gravimeter. *Review of Scientific Instruments* 70: 4131–4152.

Gumert WR (1998) An historical review of airborne gravimetry. *The Leading Edge* 17(1): 113–116.

Günter NM (1967) *Potential Theory and its Applications to Basic Problems of Mathematical Physics*. New York: Frederick Ungar Publishing Co.

Hammer S (1983) Airborne gravity is here. *Geophysics* 48(2): 213–223.

Heiskanen WA and Moritz H (1967) *Physical Geodesy*. San Francisco, CA: Freeman and Co.

Hobson EW (1965) *The Theory of Spherical and Ellipsoidal Harmonics*. New York: Chelsea Publishing Co.

Hofmann-Wellenhof B and Moritz H (2005) *Physical Geodesy*. Berlin: Springer.

Hotine M (1969) *Mathematical Geodesy*. Washington, D.C.: U.S. Department of Commerce.

Huang J and Véronneau M (2013) Canadian gravimetric geoid model 2010. *Journal of Geodesy* 87: 771–790.

Jekeli C (1988) The exact transformation between ellipsoidal and spherical harmonic expansions. *Manuscripta Geodaetica* 14: 106–113.

Jekeli C (1996) Spherical harmonic analysis, aliasing, and filtering. *Journal of Geodesy* 70: 214–223.

Jekeli C (1999) The determination of gravitational potential differences from satellite-to-satellite tracking. *Celestial Mechanics and Dynamical Astronomy* 75(2): 85–100.

Jekeli C (2000a) *Inertial Navigation Systems with Geodetic Applications*. Berlin: Walter deGruyter.

Jekeli C (2000) Heights, the geopotential, and vertical datums. Report no. 459. Columbus, OH: Ohio State University, http://www.geology.osu.edu/jekeli.1/OSUReports/reports/report_459.pdf.

Jekeli C (2004) High-resolution gravity mapping: the next generation of sensors. In: Sparks RSJ (ed.) *The State of the Planet: Frontiers and Challenges in Geophysics. Geophysical Monograph 150*, vol. 19, pp. 135–146. IUGG.

Jekeli C, Yang HJ, and Kwon JH (2012) The offset of the South Korean vertical datum from a global geoid. *KSCE Journal of Civil Engineering* 16(5): 816–821.

Kaula WM (1966) *Theory of Satellite Geodesy*. London: Blaisdell Publishing Co.

Kellogg OD (1953) *Foundations of Potential Theory*. New York: Dover Publishing.

Kenyon S and Forsberg R (2000) Arctic gravity project. *SEG Technical Program Expanded Abstracts* 19: 410–413.

Kwon JH and Jekeli C (2001) A new approach for airborne vector gravimetry using GPS/INS. *Journal of Geodesy* 74: 690–700.

Lambeck K (1988) *Geophysical Geodesy*. Oxford: Clarendon Press.

Lane RJL (ed.) (2004) *Airborne Gravity 2004 – Abstracts from the ASEG-PESA Airborne Gravity 2004 Workshop*, Geoscience Australia Record 2004/18.

Lane RJL (ed.) (2010) *Airborne Gravity 2010 – Abstracts from the ASEG-PESA Airborne Gravity 2010 Workshop*, Published jointly by Geoscience Australia and the Geological Survey of New South Wales, Geoscience Australia Record 2010/23 and GSNSW File GS2010/0457.

Lemoine FG, Kenyon SC, Factor JK, et al. (1998) *The Development of the Joint NASA GSFC and the National Imagery and Mapping Agency (NIMA) Geopotential Model EGM96, NASA Technical Paper NASA/TP-1998-206861*. Greenbelt: Goddard Space Flight Center.

Martin JL (1988) *General Relativity: A Guide to its Consequences for Gravity and Cosmology*. New York: Wiley.

Mohr PJ, Taylor BN, and Newell DB (2012) CODATA recommended values of the fundamental physical constants: 2010. *Reviews of Modern Physics* 84: 1527–1605.

Molodensky MS, Eremeev VG, and Yurkina MI (1962) *Methods for Study of the External Gravitational Field and Figure of the Earth*. Translation from Russian; Israel Program for Scientific Translations, Jerusalem.

Moritz H (1980) *Advanced Physical Geodesy*. Karlsruhe: Wichmann, Reprint 2001 by Civil and Environmental Engineering and Geodetic Science, Ohio State University, Columbus, OH.

Moritz H (2000) Geodetic Reference System 1980. *Journal of Geodesy* 74(1): 128–133.

Morse PM and Feshbach H (1953) *Methods of Theoretical Physics, Parts I and II*. New York: McGraw-Hill Book Co.

Müller C (1966) *Spherical harmonics. Lecture Notes in Mathematics*. Berlin: Springer.

Nettleton LL (1976) *Gravity and Magnetics in Oil Prospecting*. New York: McGraw-Hill Book Co.

NGS (1986) *Geodetic Glossary*. Rockville, MD: NOAA/NOS, National Geodetic Information Center, Publication of the National Geodetic Survey.

NGS (2012) *National Height Modernization Strategic Plan*. Draft Document Released to Public, November 2012, National Geodetic Survey, NOAA, Silver Spring, MD. http://www.ngs.noaa.gov/web/news/HMODPlan_PublicReview_Nov2012.pdf.

Niebauer T, Sasagawa G, Faller J, Hilt R, and Klopping F (1995) A new generation of absolute gravimeters. *Metrologia* 32(3): 159–180.

NIMA (2000) The Department of Defense World Geodetic System 1984: Its Definition and Relationships with Local Geodetic Systems. National Imagery and Mapping Agency Technical Report TR-8350.2, 3rd edn. Bethesda, MD.

Olesen AV and Forsberg R (2007) Airborne scalar gravimetry for regional gravity field mapping and geoid determination. In: *Proceedings of the Symposium of the International Gravity Field Service, 28 August–1 September 2006, Istanbul, Turkey*, Harita Dergisi (Journal of Mapping), vol. 18, pp. 277–282, General Command of Mapping, Ankara, Turkey.

Pavlis NK, Holmes SA, Kenyon SC, and Factor JF (2012) The development and evaluation of Earth Gravitational Model (EGM2008). *Journal of Geophysical Research* 117. http://dx.doi.org/10.1029/2011JB008916.

Pavlis DE, Moore D, Luo S, McCarthy JJ, and Luthcke SB (1999) *GEODYN Operations Manual*. vol. 5: Greenbelt, MD: Raytheon ITSS.

Petit G and Luzum B (2010) IERS Conventions (2010). IERS Technical Note No. 36, Verlag des Bundesamts für Kartographie und Geodäsie, Frankfurt am Main.

Petrovic S (1996) Determination of the potential of homogeneous polyhedral bodies using line integrals. *Journal of Geodesy* 71: 44–52.

Petrovskaya MS (1979) Upward and downward continuations in the geopotential determination. *Bulletin Géodésique* 53: 259–271.

Plag HP and Pearlman M (eds.) (2009) *Global Geodetic Observing System, Meeting the Requirements of a Global Society on a Changing Planet in 2020*. Dordrecht: Springer.

Rapp RH (1969) Analytical and numerical differences between two methods for the combination of gravimeter and satellite data. *Bollettino di Geofisica Teorica ed Applicata* 11(41–42): 108–118.

Rapp RH and Pavlis NK (1990) The development and analysis of geopotential coefficient models to spherical harmonic degree 360. *Journal of Geophysical Research* 95(B13): 21885–21911.

Reigber C, Balmino G, Schwintzer P, et al. (2002) A high quality global gravity field model from CHAMP GPS tracking data and accelerometry (EIGEN-1S). *Geophysical Research Letters* 29(14). http://dx.doi.org/10.1029/2002GL015064.

Rummel R, Balmino G, Johannessen J, Visser P, and Woodworth P (2002) Dedicated gravity field missions – principles and aims. *Journal of Geodynamics* 33: 3–20.

Rummel R, Yi W, and Stummer C (2011) GOCE gravitational gradiometry. *Journal of Geodesy* 85: 777–790.

Sandwell DT and Smith WHF (1996) Marine gravity anomaly form GEOSAT and ERS-1 satellite altimetry. *Journal of Geophysical Research* 102(B5): 10039–10054.

Sansò F and Rummel R (eds.) (1997) *Geodetic boundary value problems in view of the one centimeter geoid*. In: *Lecture Notes in Earth Sciences*, vol. 65. Berlin: Springer.

Sebera J, Bouman J, and Bosch W (2012) On computing ellipsoidal harmonics using Jekeli's renormalization. *Journal of Geodesy* 86(9): 713–726.

Seeber G (1993) *Satellite Geodesy, Foundations, Methods, and Applications*. Berlin: W. de Gruyter.

Sjöberg LE (1991) Refined least squares modifications of Stokes' formula. *Manuscripta Geodaetica* 16: 367–375.

Studinger M, Bell R, and Frearson N (2008) Comparison of AIRGrav and GT-1A airborne gravimeters for research applications. *Geophysics* 73(6): 151–161.

Tapley BD (1973) Statistical orbit determination theory. In: Tapley BD and Szebehely V (eds.) *Recent Advances in Dynamical Astronomy*, pp. 396–425. Dordtecht: D. Reidel Publishing Co.

Tapley BD, Bettadpur S, Ries JC, Thompson PF, and Watkins M (2004) GRACE measurements of mass variability in the Earth system. *Science* 305(5683): 503–505.

Tapley BD, Bettadpur S, Watkins M, and Reigber C (2004) The Gravity Recovery and Climate Experiment, mission overview and early results. *Geophysical Research Letters* 31(9). http://dx.doi.org/10.1029/2004GL019920.

Tapley BD, Ries J, Bettadpur S, et al. (2005) GGM02 – An improved Earth gravity field model from GRACE. *Journal of Geodesy*. http://dx.doi.org/10.1007/s00190-005-0480-z.
Telford WM, Geldart LP, and Sheriff RE (1990) *Applied Geophysics*, 2nd edn. Cambridge, U.K.: Cambridge University Press.
Torge W (1989) *Gravimetry*. Berlin: Walter de Gruyter.
Torge W and Müller J (2012) *Geodesy*, 4th edn Berlin: Walter de Gruyter.
Tsoulis D and Petrovic S (2001) On the singularities of the gravity field of a homogeneous polyhedral body. *Geophysics* 66(2): 535–539.
Wolff M (1969) Direct measurement of the earth's gravitational potential using a satellite pair. *Journal of Geophysical Research* 74: 5295–5300.
Yu J, Jekeli C, and Zhu M (2002) The analytical solutions of the Dirichlet and Neumann boundary value problems with ellipsoidal boundary. *Journal of Geodesy* 76(11–12): 653–667.
Zumberge MA, Rinker RL, and Faller JE (1982) A portable apparatus for absolute measurements of the Earth's gravity. *Metrologia* 18(3): 145–152.